Maximizing Energy Output of Wind Turbines through Novel Turbine Designs

Jacob Isaac
jmisaac@wpi.edu

Georgios Komninos
gkomninos@wpi.edu

Jose Arturo Leal Figueredo
jlealfigueredo@wpi.edu

Matthew Segui
mdsegui@wpi.edu

A Major Qualifying Project submitted to the faculty of Worcester Polytechnic Institute in partial fulfillment of the requirement of the Degree in Bachelor of Science in Mechanical Engineering.

Submitted April 25th, 2024, to:
Professor Aswin Gnanaskandan and Ahmet Sabuncu, Worcester Polytechnic Institute

Abstract

As we see an overall shift towards renewable energy sources, wind turbines have garnered a lot of interest in the recent past. With the global shift towards urbanization, the uneven heating of constructed environments can induce the formation of vertical air currents known as "thermals". This project explores the design and construction of a novel wind turbine capable of orientating its blades' axis of rotation to harvest energy from thermals optimally. We designed an optimized structural support for the assembly, a novel tilt mechanism to change the axis of the blades and developed and validated data acquisition methods to measure the torque and power generated by the turbine. CFD simulations and experimental testing were conducted to validate the design's efficacy.

Acknowledgements

The work accomplished in this paper has been made possible with the support of the following:

- Aswin Gnanaskandan
- Ahmet Sabuncu
- Jack Ryder
- Pradeep Radhakrishnan
- Peter Hefti
- Frederick Brokaw
- Mahesh Kottalgi
- Barbara Furhman
- Matthew Sweeney
- Joel Harris and WPI Washburn Manufacturing Lab Staff
- WPI Makerspace Staff

Authorship

This paper was collectively edited by all members of this MQP.

Section Header	Primary Author(s)
Abstract	All Members
Executive Summary	All Members
1. Introduction	Georgios Komninos
2. Background	
2.1 Wind Turbines	Jacob Isaac
2.2 Measuring Torque of a Rotating Shaft	Matthew Segui
2.3 Thermals Effect	Matthew Segui
2.4 Measuring Torque of a Rotating Shaft	Matthew Segui
3. Methodology	Jose Arturo Leal Figueredo and Georgios Komninos
3.1 Design Three Novel Wind Turbines that Maximize Energy Output	Jose Arturo Leal Figueredo and Georgios Komninos
3.2 Fabricate Designed Wind Turbines	Jacob Isaac
3.3 Test and Validate Novel Wind Turbines	Jacob Isaac and Matthew Segui
4. Results	
4.1 Design of Novel Wind Turbines that Maximize Energy Output	Jose Arturo Leal Figueredo
4.2 Fabricate Designed Wind Turbines	
4.2.1 Turbine	Matthew Segui
4.2.2 Mast and Structural Support	Jose Arturo Leal Figueredo
4.2.3 Tilt Mechanism	Matthew Segui
4.2.4 Instrumentation	Matthew Segui
4.3 Test and Validate Novel Wind Turbine	
4.3.1 Wind Tunnel Turbine Testing	Georgios Komninos
4.3.2 Tilt Mechanism Testing	Jose Arturo Leal Figueredo
5. Discussion	
5.1 Instrumentation	Matthew Segui
5.2 Turbine Vibration	Jacob Issac
5.3 Tilt Mechanism	Jose Arturo Leal Figueredo
5.4 Mast	Jacob Isaac
6. Conclusion	Jacob Issac
7. Broader Impacts	Matthew Segui
8. Recommendations	
8.1 Instrumentation	Matthew Segui

8.2 Tilt Mechanism	Jose Arturo Leal Figueredo
8.3 Mast and Structural Support	Jacob Isaac and Jose Arturo Leal Figueredo
8.4 Nacelle Improvements	Matthew Segui

Table of Contents

Table of Figures

Executive Summary

Wind turbines are made to capture wind energy and transform it into clean, sustainable electricity. As technology advances, wind turbines become increasingly efficient, cost-effective, and environmentally friendly, contributing to a greener, more sustainable energy landscape. They play a crucial role in reducing carbon emissions, promoting energy independence, and fostering a cleaner and more resilient energy future. A conventional single axis wind turbine harnesses the wind coming in a direction parallel to the axis of the blades (typically horizontal winds). However, in most environments vertically rising air currents, also known as thermals, are caused by localized heating on the ground. Air near the hot spot will heat up and rise due to natural convection. Over a large area, the heated air converges into a concentrated column like a tree (Angevine, 2006). These thermal winds usually combine with the existing horizontal wind and causes an inclination angle to the blade.

The goal of this project was to design, fabricate, and test a novel variable axis turbine (VAWT) that maximizes energy output by harnessing the thermal air currents. This is done by dynamically orienting the blade axis to account for the thermal current's direction. Our team used SolidWorks to design models and drawings that were to be later used and revised during our fabrication and testing periods. Models also allowed us to assess the construction feasibility of each design to reduce waste construction costs. Once we had finished our initial turbine design, our team both purchased and fabricated according to the design plan. Throughout C and D term, we conducted physical testing at WPI's Fire Protection Engineering wind tunnel. We conducted two types of testing. The first is with the turbine completely perpendicular to the wind stream, which is the standard position a turbine will have when in use. The second type of testing simulated vertical and horizontal wind vectoring and the result of these streams. We believed the

two testing types covered all forms of wind streams a turbine can experience and what the specific turbine design given was made to experience.

The housing of the turbine was made from 6061 Aluminum sheets and acrylic side panels. The drivetrain of our turbine can be broken down into four parts: blade hub, driveshaft, intermediate coupler, and generator. The mast is an essential part of our wind turbine design, crucial for providing structural support and stability to the entire system. The base was composed of 4 legs attached to the central mast in a t-shaped formation. We applied multiple reinforcements to strengthen both mast and base to maintain structural stability and dampen vibrations that resulted from head movement. This turbine's tilt mechanism consists of a vertical wind plate, horizontal and vertical extenders, and nacelle attachment points. It was found after building the first prototype that this first mechanism was not sufficient to provide enough tilting force with the current nacelle due to having its CG not at the pivot point in the y axis. Our team then redesigned the tilt mechanism to have the tilting plate closer to the pivot point to reduce the amount of counterweight needed to be placed on the front of the nacelle to bring up the combined CG. CFD testing was utilized to check if moving the plate directly behind the blades and nacelle will affect the wing's performance. The CFD showed that although behind the turbine nacelle, 2.7 N of lift can be produced in the standing position. Since our setup will be balanced around the pivot point, this will be sufficient to drive the turbine’s tilting mechanism. Instrumentation included in the wind turbine is a strain gauge-based torque transducer, voltage and current sensors, an infrared (IR) based tachometer, and Arduino Uno R3 microcontroller. Calibration of the torque sensor loosely followed the DIN 51309:2005 procedure of gradually loading and unloading the sensor in both positive and negative torque directions. Once we finished construction of the turbine and instrumentation, we performed perpendicular horizontal

wind tunnel testing. The highest average mechanical power output was during test two at 1.2 Watts with a horizontal speed of about 3.17 m/s (7 mph). To assess the functionality of our tilt mechanism, we conducted a series of tests at Higgins Labs utilizing an industrial fan to simulate thermal currents. Throughout the experimentation process, we adjusted the orientation of the fan to mimic various wind vector angles. As we adjusted the fan, we observed that an angle of 50° provided the optimal performance from our tilting mechanism.

Although the sensors installed in the turbine measured several data points from it, there were still some limitations our group faced with them. One of the larger problems faced was the significant amount of noise coming from the mechanical torque data. Different parts of the assembly vibrated while operating, causing small energy losses. Our current tilt mechanism cannot fully angle itself to the theoretical 30° angle. This issue may be attributed to the structural balance of the entire turbine. The mast, as observed during the assessment, possessed a distinctly rudimentary appearance, heavily reliant on screws and brackets for its structural integrity, making any form of manipulation, be it assembly, disassembly, or addition of components, an arduous and time-consuming task.

In conclusion, the goal of this project was to design, fabricate, and test novel wind turbine designs to maximize energy output. We were able to do this for one of the turbines, which utilized a tilt-mechanism to change the pitch of the turbine's nacelle. The turbine's tilting mechanism was seen to work in the tests we conducted and adjusted according to our simulated vertical wind vectors. The blades would rotate according to horizontal wind vectors, confirming that the unorthodox turbine setup could produce a mechanical motion. The data we obtained showed extremely low efficiency, with heavy noise and a maximum power output of about 1.9 W, as seen with our second test. We are not saying, however, that the project was a failure. We

have confirmed the tilt mechanism, the aspect which sets this turbine apart from others, works. This, and the current turbine assembly, sets the base for what future MQP teams will work with. Further on, we will provide a comprehensive list of what these teams can work on to improve the turbines design/configuration. This project's broader impact can be seen in the potential energy and environmental gains once this prototype becomes fully mature. Installation of a mature form of this design can help with grid stability and energy security in areas prone to thermal winds. In addition to the energy impacts, this technology's full maturity will also reduce the environmental impact of power generation. With improvements to wind technology, through developments like this project, and improved energy storage technology, society can reduce reliance on fossil fuels.

Although a significant amount of progress was made over the course of this project, there are many improvements that can be made to further improve the current turbine design. In order to collect more data to make better design improvements, our team recommends improving the strain gage torque sensor, more wind sensors, and event-triggered flags. To optimize the performance of the tilting mechanism, we recommend prioritizing the center of gravity (CG) optimization and weight reduction measures. To make the mast better we recommend using cheaper, light, and strong material to compose the mast. The next component that needs to be integrated into the turbine would be adding the yaw control to the nacelle support structure. This was left out in this project to focus on the pitch tilting mechanism. This yaw control system would consist of a rotating table connecting the nacelle pivot holder to the mast assembly and stabilizer fins to orientate the turbine downwind passively. One final system that was left out that should be explored is vibration sensing, suppression systems, and the implementation of solar panels on the tilting wing.

1. Introduction

This paper discusses the design, manufacturing, and testing of a wind turbine design that makes use of the thermals effect via a tilting-mechanism. To preface, we were given 3 novel turbine designs with different caveats: (i) aerodynamically actuated tilt axis (ii) servo motor-controlled tilt axis and (iii) combined horizontal and vertical axis. Some goals slightly shifted or became more specified as our project progressed, but our overall objectives stayed consistent throughout the year. The first was the designing of the wind turbine in modeling software, first as a rough idea of what we wanted, then as a fully detailed design. For this, we researched various designs for blade shapes and analyzed tilt mechanisms. Much of this initial phase also required us to properly scale down the turbine to get proportionally correct energy outputs when we tested it. Our second goal was the fabrication of the wind turbine. For this, we bought materials from sites such as McMaster-Carr and Amazon while keeping within a $1000 budget. We also calculated the size/diameter of the rotor, the frame, and the wings; the parameters for this design were based on the dimensions of the wind tunnel at Gateway. This finally leads to our third goal, which was testing the wind turbine we made. We needed to acquire data in these tests as a means of understanding how the turbine was performing. The specificities of achieving these goals, as well as the problems we encountered, are told in detail throughout this paper.

2. Background

Wind turbines are devices designed to capture the kinetic energy of wind and convert it into electrical power. They have led the way in the development of renewable energy technology, providing a sustainable and clean source of power. Wind energy has gained general recognition as a key solution in addressing the global challenges of climate change and the transition to more sustainable energy sources. Over the years, wind turbines have evolved from small, localized structures to massive wind farms with towering turbines capable of generating significant amounts of electricity. As technology advances, wind turbines become increasingly efficient, cost-effective, and environmentally friendly, contributing to a greener and more sustainable energy landscape. They play a crucial role in reducing carbon emissions, promoting energy independence, and fostering a cleaner and more resilient energy future.

2.1 Wind turbines

Wind turbines are made to capture wind energy and transform it into clean, sustainable electricity. The tower, nacelle, rotor blades, and control systems are among the essential parts of these turbines, as seen in Figure 1. The nacelle holds the gearbox, generator, and other essential components, while the tower's height enables the rotor blades to access higher wind speeds. Rotation is created by wind passing over the turbine blades, producing an aerodynamic lift force that turns the rotor. The specific aspect of these wind vectors that create lift is that they act perpendicularly against the airfoils (Leishman, 2022). Without this aspect, an average vertical or horizontal axis wind turbine would not be able to function properly.

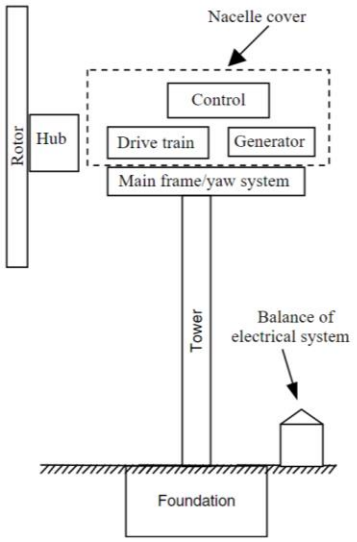

Figure 1: Horizontal Wind Turbine Schematic (Manwell et al., 2009)

The rotor blades, which are frequently composed of strong yet lightweight materials like carbon, capture the kinetic energy of the wind. The rotor, which is coupled to a gearbox, rotates as the wind drives the blades and increases rotational speed. The generator is subsequently powered by the gearbox, which transforms the rotational energy into electrical energy.

The reason why turbines move the way they do is a result of two different scientific principles. The first is Newtons 3rd law, which states that every action has an equal and opposite reaction. In this case, the air pushing against the blade causes the reaction of the blade being deflected. The second revolves around Bernoulli's principle, in which the blade is designed so that the air traveling on the downwind side of the blade is traveling faster than on the upwind side. The differences between these pressures result in the blade being "lifted" in the direction of the curve of the blade. The key purpose of every blade design, or airfoil, is then the maximization of lift force and the minimization of drag.

While there is not one single way to design an airfoil, there is a multitude of commonly agreed upon strategies to achieve a successful turbine blade. Among these include designing a blade which is composed of lightweight and smooth materials, as doing the opposite will

inevitably increase drag force. The primary ways to increase lift force comes with the blades angle relative to the plane of rotation and of apparent wind, which is aimed at being designed between 10-20 degrees. The other way to increase lift force is to design a blade with a small flat tip, and an angled broad root. This, of course, is not a complete list of factors to take in with blade design, but these are the biggest issues we kept in mind as we went into the project (Leishman, 2022).

2.2 Thermals Effect

Vertically rising air currents, also known as thermals, are caused by localized heating on the ground. Air near the hot spot will heat up and rise due to natural convection. Over a large area, the heated air converges into a concentrated column similar to a tree (Angevine, 2006). As long as the rising air is warmer than its surroundings, the air will continue to rise. Once the rising air is cooler than the surrounding air, it will fan out and sink due to being less dense than the heated air. This creates a circulating air current of rising and sinking air, as seen in Figure 2.

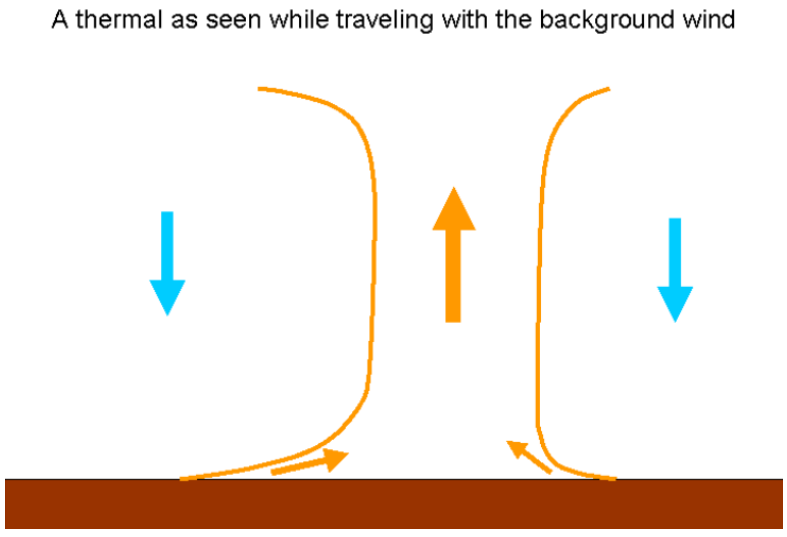

Figure 2: Thermal Side Cross Section (Angevine, 2006)

Thermals are also affected by surrounding wind currents. When subjected to horizontal wind current, the wind mixes with the rising heated air and causes the air to rise at an angle

instead of vertically (Angevine, 2006). When the wind is sufficiently strong, thermals will become smaller and weaker. This is caused by the strong mixing of cool wind air and rising heated air to become equal to the surrounding air temperature faster, thus causing the locally heated air to sink until it is sufficiently heated. A similar effect happens when there is insufficient sunlight to heat the ground, which can cause a temperature difference.

Solar updraft tower power plants take advantage of the thermal effect to harvest energy from the created updrafts. They mainly consist of a thermal collector surface that heats up from solar radiation, a turbine to generate power, and a chimney/tower to funnel air to the turbine (Zhou and Xu, 2014). This type of power plant is appealing to areas that are relatively flat and receive an abundant amount of sunlight, such as a desert. The principle of these power plants has also been adapted to urban settings where the thermal collector surface is asphalt (García and Partl, 2014).

2.3 Design and Operational Parameters of Wind Turbines

Basic wind turbine design relies on the principle of converting the kinetic energy from the air into work used to spin a generator. To achieve this, several factors play into the design of wind turbines to optimally harvest available energy. Starting with the wind itself, the theoretical maximum power that can be generated from the wind can be expressed as

$$\dot{W}_{available} = \frac{1}{2}\rho A V^3$$

where ρ is the air density, A is the swept are of the turbine blades, and V is the measured wind velocity (Kanoglu et al., 2019). This equation shows the first two parameters that can be manipulated to increase power generation: the swept diameter and the incoming wind speed. The swept diameter can be increased by increasing the length of the blades. Increasing the incoming wind speed can be done in two ways. The first is moving to a region that is prone to higher wind

speeds, also known as having a higher wind resource. The second is increasing the height of the mast. This can be calculated with the relationship

$$\frac{V}{V_0} = \left(\frac{h}{h_0}\right)^{\alpha}$$

where V is the wind speed at height h, V_0 is the wind speed at height h_0, and α is the friction coefficient of the ground (Kanoglu et al., 2019). The value of α ranges from 0.10 for a smooth ground to 0.40 for a highly urbanized environment.

The direction the wind comes in from has an effect on the efficiency of a wind turbine. Traditional wind turbines can account for horizontal misalignment with yaw control systems that will pivot the turbine nacelle to be aligned with changing wind directions, however, there is limited literature on the use of pitch control systems to account for vertical misalignment produced through thermals. As seen in Figure 3, if vertical misalignment were to occur, there would be potential power losses proportional to the cubic sine of the angle that the wind originated coming from. Annoni et al. (2017) explored this pitch concept in the form of wake production in a farm setting and found an overall increase in power gains, however, the tilt study was not studied in depth on the gains of individual turbines.

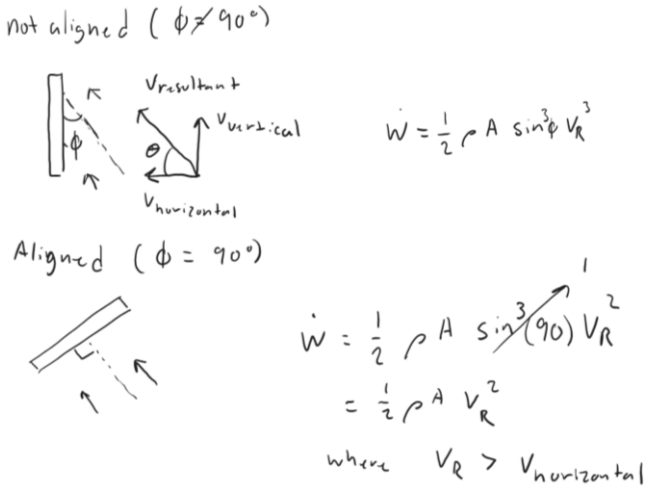

Figure 3: Vertical Misalignment Diagram

To transform this available energy, we must use machinery where various power losses can be found. Factoring this into the available energy from the wind equation, the actual energy harvest can be expressed as

$$\dot{W} = \frac{1}{2}\eta_{overall}\rho A V^3$$

where now $\eta_{overall}$ represents efficiency of all the components of a turbine (Kanoglu et al., 2019). These include the blades, gearboxes, generators, and other drivetrain components which all work together to produce electrical power. It is important to note that these efficiencies have an upper limit known as the Betz limit at around 0.5926 (Kanoglu et al., 2019). This means that in idealized turbine design will only harvest around 60%, meaning that further drops in efficiency will come from design decisions and environmental effects such as swirls. To avoid these efficiency stack ups, we can focus on the first point of contact between the incoming wind and turbine: the blades and initial drivetrain section. Measuring work done at this point will minimize energy loss that a designed turbine will experience from its other power generating components, relying on the efficiency of the blades to catch the wind.

2.4 Measuring Torque of a Rotating Shaft

Torque is an important value to measure since it is proportional to the amount of power a turbine can produce as previously stated. Power with respect to torque can be written as $P = T*\omega$ where T is the torque and ω is the rotational velocity acting on the shaft of the turbine. There are multiple ways to measure torque as out lined by Schicker and Wegener (2002):

- Torque from electrical power
- Reaction (static) torque
- In-line torque sensors
- Torque from torsional stress

Torque derived from electrical power can be found by dividing the power produced from a generator by the angular speed of the generator shaft. This method of torque measurement is not reliable because of several factors that decrease the efficiency of the generator, decreasing the accuracy of the measurement (Kang and Meneveau, 2010).

Reaction torque can be found by multiplying an applied force by the distance way from in line measurement point. This concept is similar to the way a torque wrench takes measurements. There are many literatures that use variations of this technique. Most of them consist of a generator that is able to pivot until it is stopped by a lever arm (Kang and Meneveau, 2010). This lever arm applies presses down on a load cell that outputs the force applied by the arm (Figure 4). By this principle, users can measure both mechanical and electromagnetic torque applied to a turbine shaft.

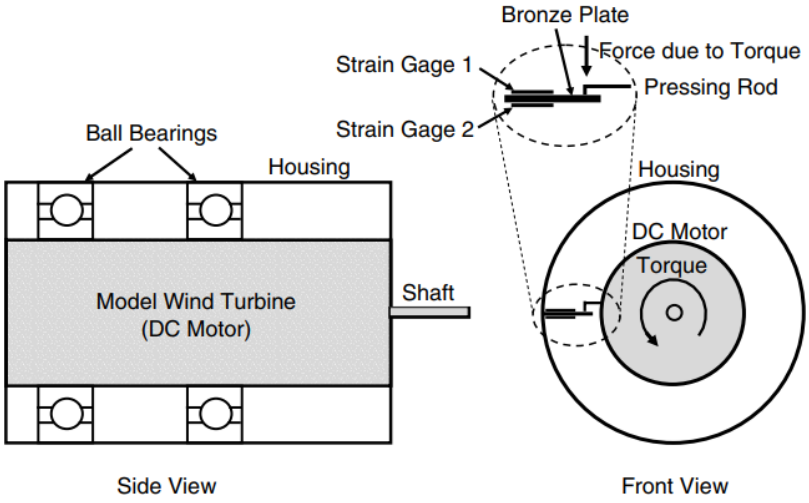

Figure 4: Reaction Torque Measuring Setup (Kang and Meneveau, 2010)

In-line torque sensing is done by connecting the drive and driven shafts on opposite ends of a torque sensor. Depending on the various measurement probes integrated into the device, different kinds of torque can be measured from the one sensor. This method of measuring torque is the most simple since all of the calculations are done with the sensor (He et al., 2022).

The final way to measure torque is through torsional strain. This type of strain comes by applying a constant torque in opposite directions of a shaft, causing it to have a twisting deformation. The use of strain gauges can measure the deformation and can be converted into the torque that was acting on the shaft. An example of the use of this technique can be seen in Figure 5. In their setup, measurement components were attached to the rotation shaft to obtain torsional strain readings. They then used the following equation to convert the signal obtained by the Wheatstone bridge created by the strain gauges to find torque applied to the shaft:

$$Q_{shaft} = U_A \frac{\pi E D^4}{16 U_E k D (1 + v)}$$

where U_A is the supply voltage, U_E is the bridge output, E is the Young's modulus of the shaft, D is the shaft diameter, k is the gauge factor of the strain gauges, and v is Poisson's ratio. This equation uses small deformation theory to transform shear strain measured by the strain gauges to torque applied to the shaft. A derivation of this equation can be found in Appendix A: Derivation of strain gauge deformation to torque on a shaft.

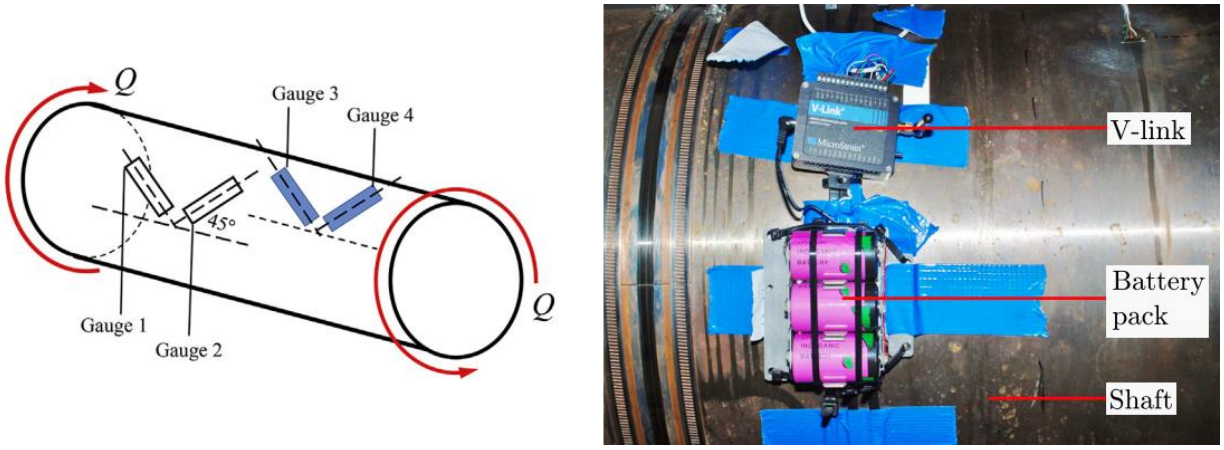

Figure 5: Torsional Stress to Torque Setup (De Waal et al., 2018)

Out of the mentioned methods for measuring torque, our team decided to use the strain gauge method. Our reasoning behind this decision is because the strain gauge option is least

sensitive to inefficiencies within our budget limitations. The electrical and reaction torque methods are both sensitive to electrical and mechanical losses, respectively. Inline torque sensors are also not an option due to their high cost ranging the thousands of dollars. The strain gauge method only relies on elastic deformation, meaning if the correct shaft material is selected, torque can be measured with high accuracy.

3. Methodology

The goal of this project was to design, fabricate, and test three novel turbine designs that maximize energy output. To achieve this goal, the following objectives were:

1. Design three novel wind turbine designs that maximize energy output
2. Fabricate designed wind turbines
3. Test and validate novel wind turbines

In the end, limited by time and budget constraints, we designed, fabricated, and tested one of the turbines.

3.1 Design Three Novel Wind Turbines that Maximize Energy Output

Our team originally planned to design three wind turbines that make use of the thermals effect. The core feature of all three turbines is the ability to position itself in a way to harvest both horizontal and vertical wind currents.

The first design, which we will refer to as the thermals powered wind turbine, takes advantage of two things. The first is the horizontal winds which already exist in its environment via wind currents. The second is thermal, the vertically flowing air resulting from light heating the pavement near the turbine. The resultant of these two currents is also utilized to generate electricity in the turbine. On a normal day, the turbine will begin with its rotation axis positioned horizontally, and a controller will change its axis as the day goes on based on the thermal velocity obtained from an anemometer and the horizontal wind velocity. If horizontal wind velocity is clocked at being very low, the turbine will be positioned at a 90-degree angle and the thermals will then power the turbine. If thermal velocity and horizontal wind velocity are relatively equal, the controller will position the axis to 45-degrees to maximize electricity output.

If thermal velocity is very low, then the controller will keep the axis at its original horizontal angle.

The second design is called the Tilt Axis Wind Turbine (TAWT-4) which is designed to harness the often-underutilized energy resource of rising air currents or thermals. These thermals, formed because of the sun's heating effect on specific surfaces, create an upward wind current which brings up an interesting opportunity for renewable energy generation. The TAWT-4 distinguishes itself by not only recognizing the potential of thermals but by also embracing the adaptive nature of its operation. This innovative wind turbine can seamlessly adapt to varying environmental conditions, particularly in response to incoming air currents. Its hallmark feature is the dynamic adjustment of its axis orientation, which allows it to align itself with the prevailing wind direction achieving about up to 60-degree angle of inclination. This adaptive mechanism ensures that the TAWT-4 operates at peak efficiency throughout the day, taking advantage of thermals when available and changing direction depending on the incoming air currents.

The third design introduces the "VAWT-HAWT," an innovative pair of wind turbines, representing a substantial leap in wind energy technology. A vertical-axis wind turbine (VAWT) and a horizontal-axis wind turbine (HAWT) are smoothly combined in this innovative hybrid system to form a solid framework that improves electrical energy production. This innovative design is based on the idea of combining the potential of two main airflow directions: the traditional horizontal winds and the less explored but essential vertically rising air currents, caused by thermals due to the sun's heating influence. The concept tries to harness not just one, but both common airflow patterns by a deft integration of a HAWT onto a normal VAWT, providing a more reliable and resilient power generating process. By adjusting to the many wind

conditions that a location may experience, the VAWT-HAWT system has the ability to maximize energy output. This adaptability, which supports the urgent global switch from fossil fuels to cleaner energy sources, is essential for meeting sustainability goals and mitigating the effects of climate change. All in all, the VAWT-HAWT system represents innovation and environmental awareness by providing a novel way to enhance electricity production while minimizing environmental impact. This creative answer serves as evidence of human innovation, advancing us toward a future when clean and abundant energy is not just a fantasy but a concrete reality as the world unites in the shared search for renewable energy. For future generations, this development creates a world that is more vibrant and sustainable.

Of these three designs which were provided to us by WPI alumni Jack Ryder, we decided that the turbine which would take priority was the Tilt-Axis Wind Turbine due to it being the least dependent on electronics. As electrical work is not favorable for us from an organizational aspect; keeping all wires easily organized and housed. There is also the aspect of all four members of our group being Mechanical Engineering majors, and as such don’t have enough electronics experience needed for an electrical-based project. Our team used SolidWorks to design models and drawings that were to be later used and revised during our fabrication and testing periods. Models also allowed us to assess the construction feasibility of each design to reduce waste construction costs.

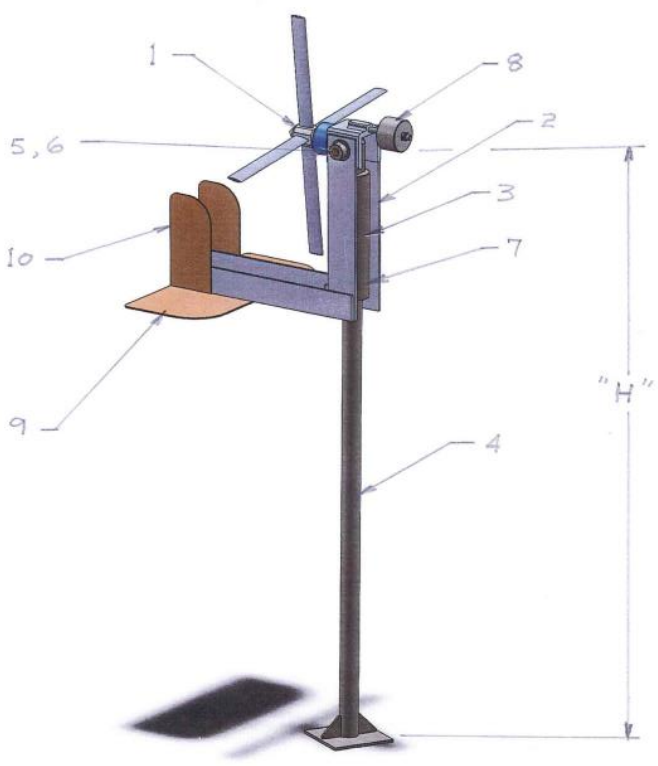

Bill of Materials

1	Wind Turbine
2	Main Frame
3	Pivot Frame
4	Mast
5	Axle
6	Bearing Housing
7	Mast Bearings
8	Counter-Weight
9	Wing
10	Rudder

Figure 6: a. Original Design and b. Bill of Materials

3.2 Fabricate Designed Wind Turbines

Once we had finished our initial turbine design, our team both purchased and fabricated according to the design created in objective 1. Given this project's budget, cost-saving techniques ensured a high-quality turbine prototype of the concepts we are testing.

For the working turbine components, we purchased the Vevor 5-blade 400W wind turbine and disassemble it into its turbine blades and generator. From these components, we fixed our measurement sensors to the rotor shaft connecting the blades to the generator. Sensors included an IR sensor-based RPM sensor, a voltage divider-based voltage sensor, and a Hall effect-based current sensor. We then constructed an appropriate nacelle using ¼” aluminum panels as well as 2 acrylic side plates to protect these internal components and improve the aerodynamics of the wind turbine.

3.3 Test and Validate Novel Wind Turbines

We looked at both torque generated by the blades transferred to the rotor shaft, as well as the effectiveness of the tilt-mechanism of the turbine. In the project, our group focused mainly on physical testing and simulation-based testing. This happened concurrently, and for physical testing we utilized one of the resources offered here at WPI, the wind tunnel. For simulation testing we used SolidWorks Simulation and utilized the FEA (Finite Element Analysis) feature.

Throughout C and D term, we conducted physical testing at WPI's Fire Protection Engineering wind tunnel. We consulted a paper by He et al. (2022) in regard to how we tested our turbine. There are several factors that were also taken into consideration with wind turbine testing. To reduce the impact of the blockage effect, we kept the obstructed area of the wind tunnel to less than 10% (He et al., 2022). To have the same operating conditions as the full-scale turbine, a dynamic similarity calculation was performed to ensure proper scaling of the prototype and adherence to the 10% blockage limit. Inflow velocity was determined via an anemometer tested at about the middle of the wind tunnel cross-section at wind tunnel entrance. (He et al., 2022).

We conducted two types of testing. The first is with the turbine completely perpendicular to the wind stream, which is the standard position a turbine will have when in use. The second type of testing simulated vertical and horizontal wind vectoring and the result of these streams. . We believed the two testing types covered all forms of wind streams a turbine can experience and what the specific turbine design given was made to experience.

Figure 7: a. Fixed Perpendicular Testing, b. Tilting Testing

Torque readings were collected, as well as collect rotational speed either by an isolated counter and incorporation via a function into our torque acquisitor (He et al., 2022). The product of the torque and rotational speed gave us mechanical power, in which we made inferences about the efficiency of the turbine. This comes from the fact that mechanical power is directly proportional to electrical power. The way we collected torque data was through a full strain gauge Wheatstone bridge arrangement on the drive end of the turbine shaft. All data acquisition devices were attached to the rotating shaft and extracted during testing. As for simulation testing, we once again conducted finite element analysis (FEA) using SolidWorks Simulation. Using this we compared strain to the voltage which was being produced by the Wheatstone bridge.

4. Results

The following section details the realized design, fabrication, instrumentation, and testing of our novel wind turbine.

4.1 Design of Novel Wind Turbines that Maximize Energy Output

Our team carefully assessed the three wind turbine designs and determined that the Tilt Axis Wind turbine (TAWT-4) would be the most prioritized to build because of its unique design and ability to maximize energy output. The design aims to create a balance between incorporating some of the key performance features we were aiming for and maintaining simplicity in construction. The TAWT-4 sets itself apart by identifying the untapped energy source of rising air currents or thermals, which offers a special chance for renewable energy production.

The TAWT-4 design process started with a lot of study and SolidWorks modeling. As a result, we created computer-aided design (CAD) models of the turbine's structural support, tilt mechanism, nacelle, and rotor blades. We saw and assessed the structural integrity, aerodynamics, and operation of the turbine before manufacture by utilizing SolidWorks.

We included CAD images and drawings of the TAWT-4 to supplement the design process and give visuals of the turbine's parts and assembly. Throughout the fabrication and testing phases, these illustrations proved to be invaluable resources for clarifying design concepts and guaranteeing team coherence.

All things considered, the TAWT-4's design was a team effort that blended technical concepts, computer modeling, and creative thinking to produce a wind turbine that was maximized for energy production. We advanced to the fabrication stage with a strong basis in design, excited to realize our idea and confirm its functionality through testing. CAD of the Full assembly can be found in Figure 8.

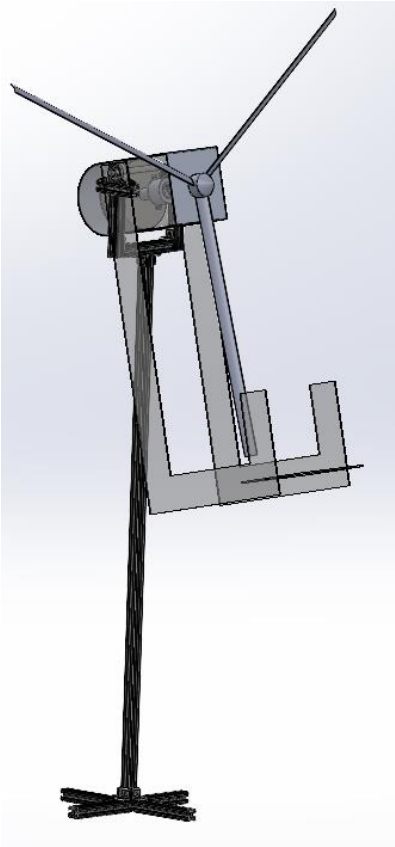

Figure 8: Full TAWT- 4 Turbine CAD Assembly

4.2 Fabricate Designed Wind Turbine

The following section will detail the fabrication of our wind turbine. The turbine's fabrication was split into four sections: the turbine itself, mast and structural support, tilt mechanism, and instrumentation.

4.2.1 Turbine Nacelle and Machinery

From the created CADs, we fabricated our designed turbine. The housing of the turbine, as seen in Figure 9, was made from 6061 Aluminum sheets and acrylic side panels. Aluminum was used to the majority of the housing since we can achieve a curved surface, helping with the aerodynamic performance of the turbine nacelle. This was formed using rollers in WPI's Washburn Manufacturing Lab. Laser cut acrylic was used as side panels to allow our team to

visually inspect the rotating machinery of the turbine. Additional 3D printed parts and laser cut acrylic was used to hold various drive train components in place within the housing.

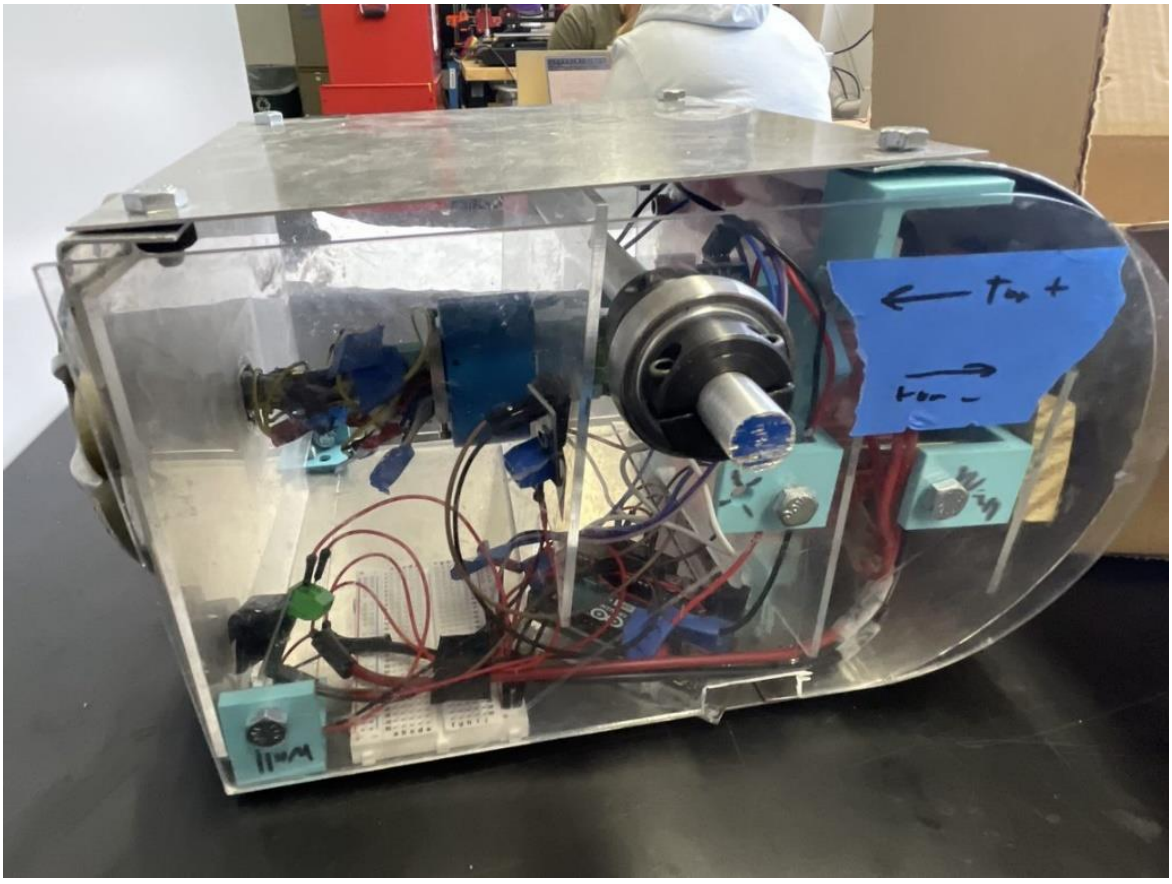

Figure 9: Turbine Housing

The drivetrain of our turbine can be broken down into four parts: blade hub, driveshaft, intermediate coupler, and generator. The blade hub reused the original hub and blades from the Vevor 400W 5-blade Wind Turbine. Additions made to the hub were blade extenders to allow the blade geometry to not get obstructed by the new housing. In addition, a hexagonal hub connector was created to attach to the driveshaft of our turbine. This hub connector was originally made of PLA, however, was changed to carbon fiber reinforced nylon to improve strength and durability. Other additional parts added by our team were 3D printed out of various polymers depending on the mechanical properties needed.

Figure 10: Turbine Hub, Rotor, and Blades

Attached to the hub connection is main driveshaft of our turbine. It is made of a keyed 2024 Aluminum due to its low elastic modulus which aids in our mechanical torque instrumentation which will be discussed in section 4.2.4 Instrumentation. The slip ring is also attached to the driveshaft to allow for some instrumentation components to rotate with the shaft and other to stay stationary. A sheet of acrylic was used to hold the slip ring in place and add structural stability to the middle section of the turbine.

At the end of the main driveshaft, a coupler is needed to join the blade driveshaft to the generator. At first, a ridged coupler was 3D printed and used to connect the two points together, however, it did not allow for the turbine to spin under wind load. A jaw coupling was then used to join the two shafts together. This type of coupling was used to account for misalignment between the drive and driven shafts. The connector on the generator side was printed out of ABS in order to reduce galling between the coupler and the threaded generator shaft.

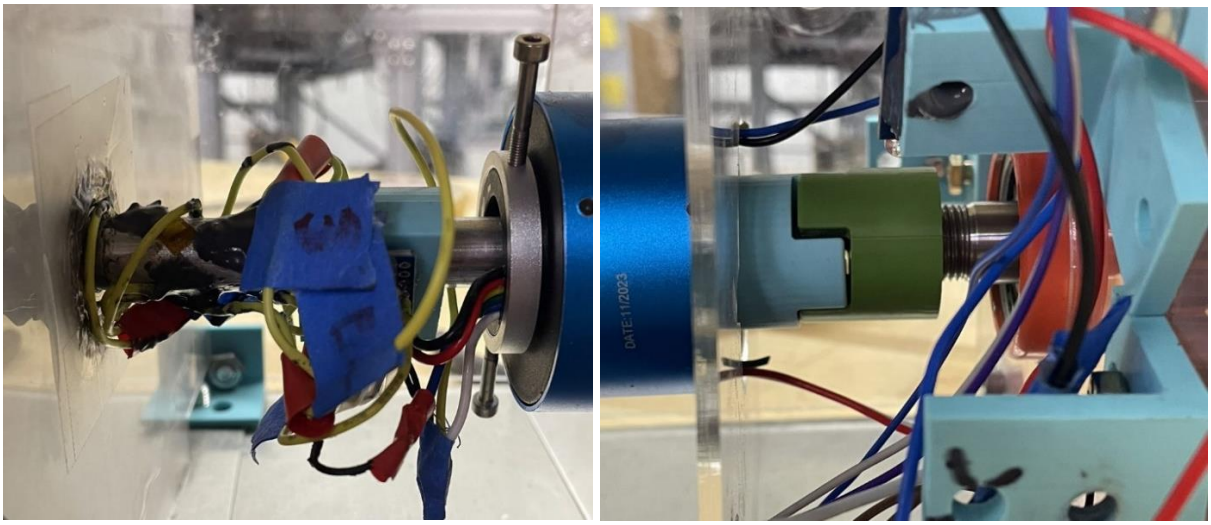

Figure 11: Driveshaft Components Containing the a. Torque Sensor and b. Jaw Coupler

At the end of the drivetrain is the turbine's generator. This was the same generator that was on the Vevor wind turbine and was removed from the original housing to reduce the size and weight of the turbine. It is a 400 W three-phase alternating current (AC) generator. To allow for a "calibration mode" on our turbine, an acrylic plate was added to the back side of the generator to install a fastener to stall movement of the generator's magnetic rotor.

4.2.2 Mast and Structural Support

The mast is an essential part of our wind turbine design, crucial for providing structural support and stability to the entire system. Fabricated with careful attention to detail, the mast was engineered to withstand a variety of wind conditions while ensuring resilience and reliability. Our material selection process prioritized factors such as strength-to-weight ratio and cost-effectiveness, aligning with our project's goal of balancing performance and affordability.

The fabrication process began with thorough planning and design, where precise specifications and drawings were generated to guide production. Utilizing SolidWorks software allowed us to create a comprehensive overview of the turbine assembly, incorporating the mast to ensure correct alignment and integration with other components.

We aimed for dimensional precision throughout the fabrication of our mast, making sure we use the right machining methods to achieve the required parameters for the mast components. We based our machining requirements utilizing the drawing from our scale dimensions, which we obtained from the original design. This allowed us to ensure accuracy and consistency in fabrication of the mast to incorporated into the turbine system fulfilling the required alignment to maintain structural balance and facilitate optimal transfer of wind currents to the rotor blades.

Mounting the nacelle, rotor blades, and other critical components over the mast demanded proper positioning and reinforcement to ensure stability and balance during operation. Multiples testing were conducted to evaluate the structural performance of the manufactured mast, confirming its ability to support the turbine system effectively. Adjustments were made to counterbalance the combined weight of the housing and blades, incorporating lateral supports and wooden guides at the base of the turbine to mitigate vibrations during operation.

As for the mast and base more broadly, the design for this changed considerably over the project. Our original design had one piece of t-slot aluminum acting as the mast, which we were assuming would support the weight of the assembled turbine head. The base was composed of 4 legs attached to the central mast in a t-shaped formation. However, early in our testing, we realized that the weight of the nacelle was far too great for the mast to support, as evident by the buckling we observed when the first iteration was fully put together. We applied multiple reinforcements to strengthen both mast and base to maintain structural stability and dampen vibrations that resulted from head movement.

The first adjustment we made was to add two more pieces of t slot aluminum connecting the base and supporting the weight of the turbine head. Along with this was two shorter pieces of

t-slot aluminum attached perpendicularly to the front and back legs and would attempt to prevent the turbine from rocking in the assembly's pitch direction.

Figure 12: Initially Redesigned Mast

However, there was another issue with the design which prevented it from working. The nacelle's weight was still causing the top of the mast to buckle, thus misaligning, and preventing the blades from rotating. To resolve this, we attached pieces of wood to the top via screws so that the top would remain straight, and the nacelle aligned. We added two pieces each to the front and back of the outermost t-slot beams.

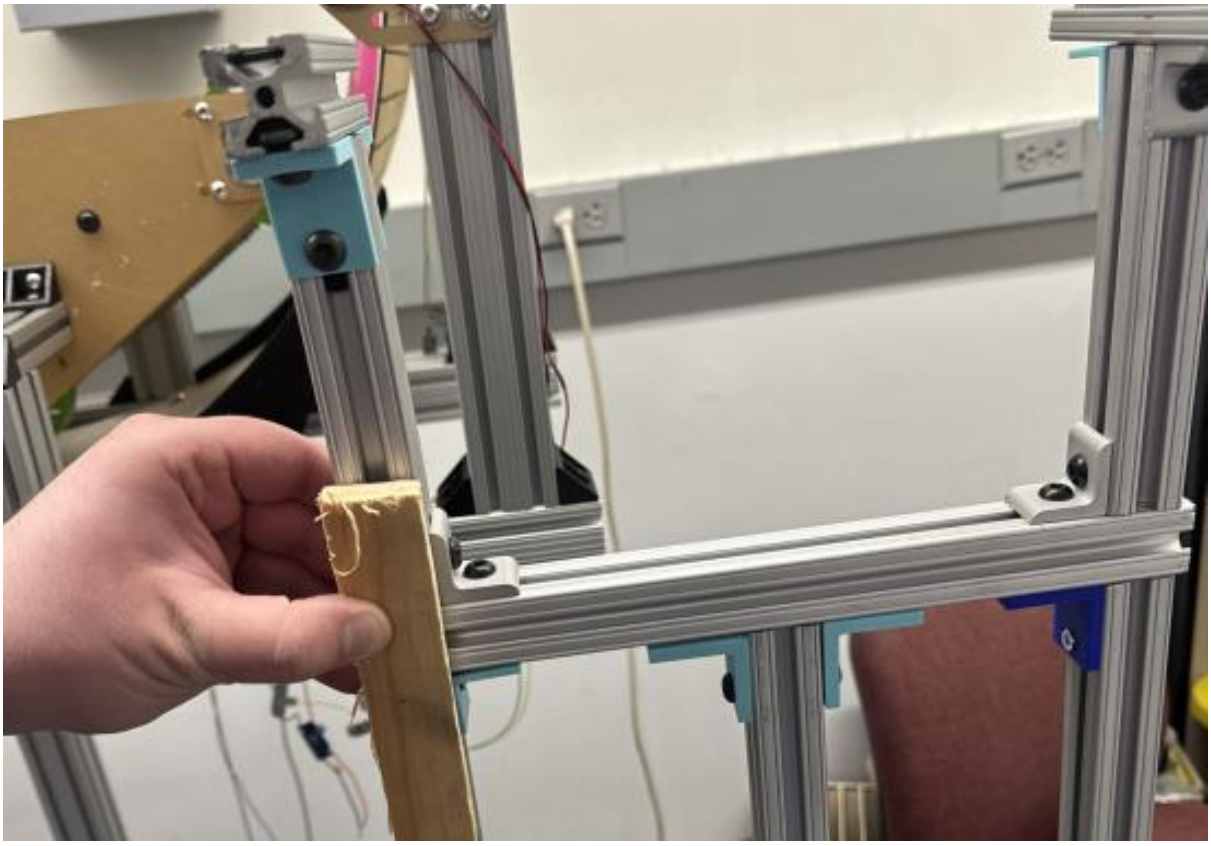

Figure 13: Wooden Mast Supports

This design worked well in maintaining the turbine assembly's straightness, and we were able to get the blades to spin. But we soon found another issue from what we initially thought of as success. The fast movement of the turbine blades caused a great vibration, which resulted in the entire mast shaking and rocking about the base. Our solution to this was using 2x4 pieces of wood to provide support from the base and prevent the mast from rotating in the pitch and roll directions. 2 large pieces of 2x4 had their edges cut at 45-degree angles, then screwed into the central mast and front and back of the base legs. 2 more smaller pieces of 2x4 were attached from the edge of the side base legs and screwed into the sides of 2 outer t-slot aluminum beams.

a. b.

Figure 14: Base Leg Supports a. Back View and b. Side view

4.2.3 Tilt Mechanism

The tilt mechanism of this turbine consists of a vertical wind plate, horizontal and vertical extenders, and nacelle attachment points. The vertical wind plate consists of a flat plate that will have thermals air pressure push against it to provide a tipping force on the turbine nacelle, positioning it in an optimal angle for energy harvesting. In order for the tilt mechanism to function properly, the pivot point about which the nacelle will have pitch adjust ability is critical. A free body analysis, as seen in Appendix B: Tilt mechanism Free Body Diagram Analysis, was preformed to reveal that the farther away the pivot point was from the center of gravity (CG), the stronger thermals must be in order to provide adequate tipping force. The first prototype of the tilting mechanism can be seen in Figure 15.

Figure 15: First Tilt Mechanism Iteration

It was found after building the first prototype that this first mechanism was not sufficient to provide enough tilting force with the current nacelle due to having its CG not at the pivot point in the y axis. When looking from the side, we needed to have the CG of the combined body of the nacelle and tilting mechanism. Our team then redesigned the tilt mechanism to have the tilting plate closer to the pivot point to reduce the amount of counter weight needed to be placed on the front of the nacelle to bring up the combined CG as seen in Figure 16. By doing this, a smaller counter weight can be used that is closer to the nacelle and will obstruct less of the frontal area of the turbine blades.

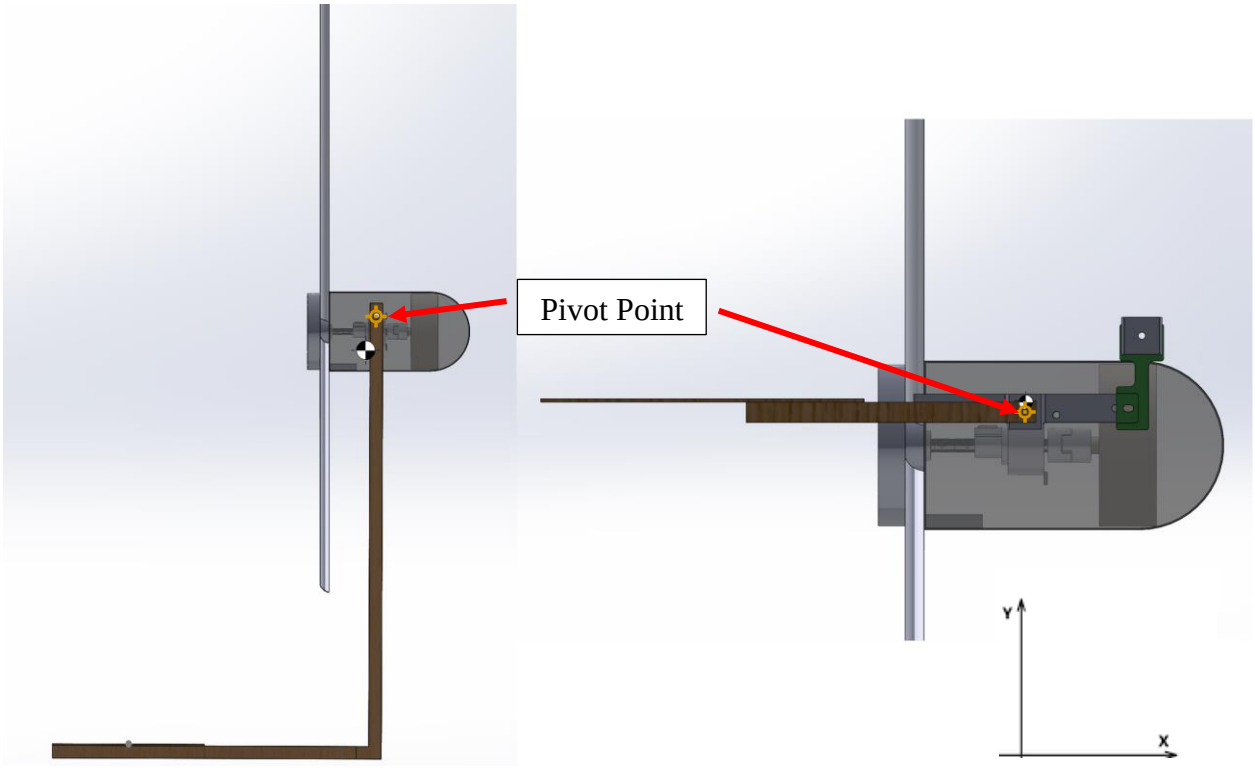

a. b.

Figure 16: CG Differences Between the a. Original Design and b. Redesign

CFD testing was utilized in order to check if moving the plate directly behind the blades and nacelle will affect the performance of the wing. This was done in with SolidWorks' Flow Simulation. Air was used as the fluid and a bounding box was placed around the CAD of the redesigned turbine. The flow velocities were set at 3 m/s in the vertical direction and 6 m/s in the horizontal direction. A streamline plot can be seen in Figure 17. The CFD showed that although behind the turbine nacelle, 2.7 N of lift can be produced in the standing position. Since our setup will be balanced around the pivot point, this will be sufficient to drive the turbine's tilting mechanism.

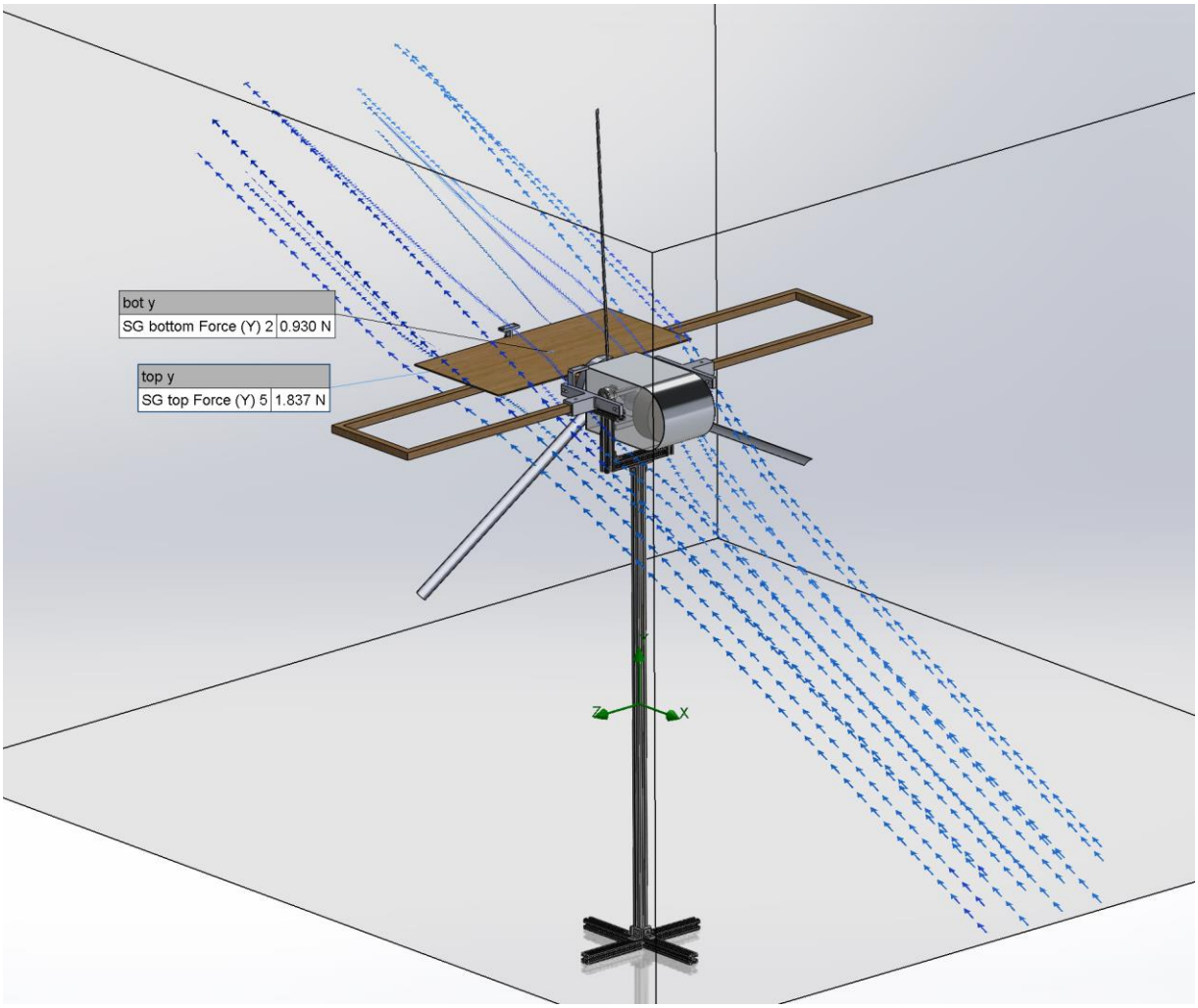

Figure 17: CFD Simulations

The constructed tilt mechanism used 0.75-inch square wood dowels, 3D printed support structures, and had a wing that was 12” x 24”. The wing had holes cut out and then was wrapped in plastic to reduce weight while maintaining its lift functionality. To counter balance the wing, a 1.2kg counterweight was used made out of mass blocks. Tension cables and a support beam were also included to support and reduce the deflection of the tilting mechanism. The final assembled tilt mechanism can be seen in Figure 18.

.

a.

b.

Figure 18: Fully Assembled Tilt Axis Wind Turbine a. Front View, b. Back View

4.2.4 Instrumentation

Instrumentation included in the wind turbine is a strain gauge-based torque transducer, voltage and current sensors, an infrared (IR) based tachometer, and Arduino Uno R3 microcontroller. The strain gauge torque transducer consists of a Wheatstone bridge, an analog-digital-converter (ADC), and slip ring. The Wheatstone bridge was affixed to the turbine's drive shaft after the rotor hub in a full-bridge configuration using 4 strain gauges in an arrangement similar to *Figure 5*. The Wheatstone bridge was connected to an ADS1115 16-bit ADC to convert the analog signals produced by the bridge to digital. Instead of using wireless data like Waal et al., our team decided to use a 6-circuit high speed electrical slip ring from ATO in order to transfer data from the strain gauges rotating on the shaft to our Arduino microcontroller attached to the turbine housing. The slip ring does this by having contact rings on the rotating part of the slip ring assembly and individual contacts on the stationary assembly. The wiring diagram for this sensor can be seen in Figure 19.

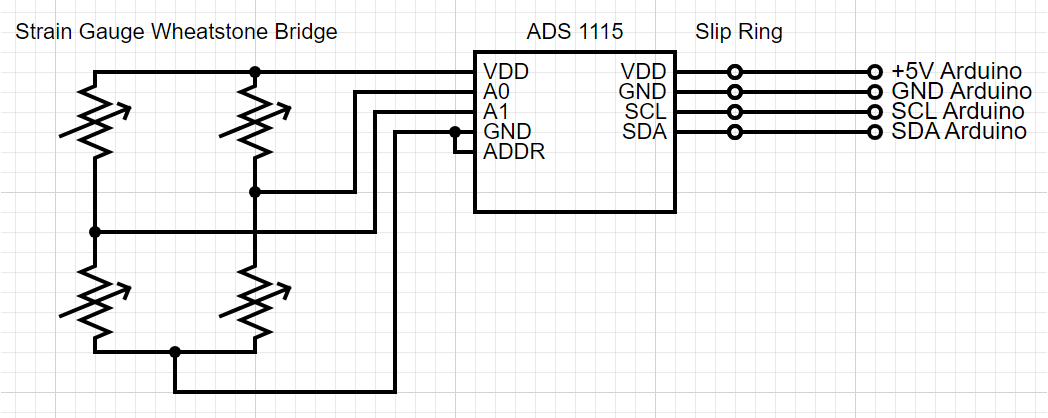

Figure 19: Strain Gauge Torque Transducer Circuit Diagram

Calibration of the torque sensor loosely followed the DIN 51309:2005 procedure of gradually loading and unloading the sensor in both positive and negative torque directions. A bolt was used to fix the generator side of the turbine to have a fixed load on the torque sensor. Masses ranging from 100g to 602g were used and placed 0.04m way from the center of the rotor shaft. Figure 20 shows the calibration curve obtained with an R^2 value of 0.9908.

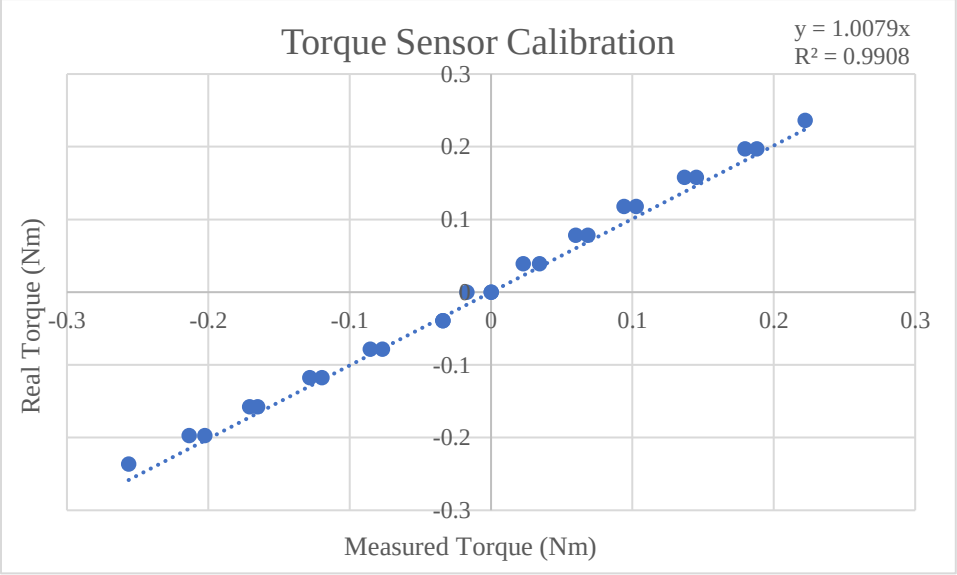

Figure 20: Calibration Curve

To validate our results from our strain-based torque transducer, we collected the power output and rotational speed of our turbine's generator. Power generated was calculated by

multiplying the measured DC voltage and current produced by the included 3-phase generator from the Vevor wind turbine. To convert the 3-phase generator to DC, we used the included wind controller and measured the output from the terminals that would traditionally connect to an energy storage device. To measure voltage, a voltage divider module was used with a 30K and 7.5K ohm resistor setup that probed the positive and negative terminals of the wind controller output. To measure current, an ACS712 hall effect based current sensor module was used by connecting the positive and negative leads of the wind controller output to complete the circuit. The analog signals produced by the voltage and current sensor modules were processed by the Arduino's onboard ADC and processed in code. The diagram for this wiring can be seen in Figure 21.

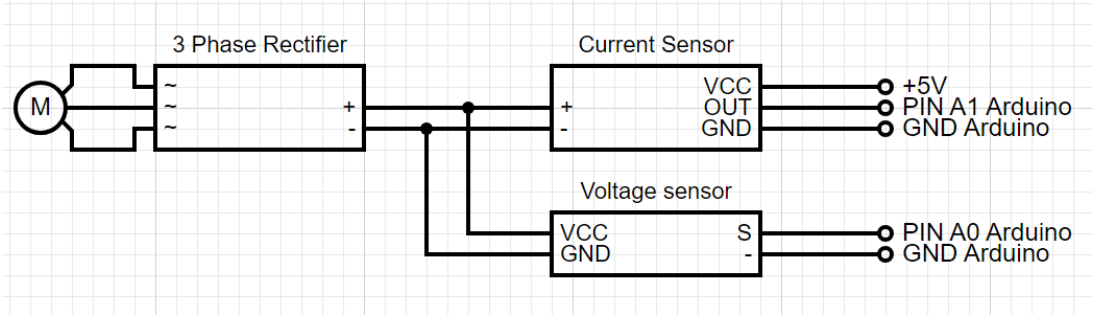

Figure 21: Generator Power Sensing Circuit Diagram

To obtain the rotational speed of the generator shaft, an IR proximity sensor module was used to measure how many revolutions are made every minute (RPM). Reflective tape was used to reflect the IR light emitted from the IR diode back to the IR receiver. Every time the IR receiver detects reflect IR light, a pulse is emitted by the proximity sensor which was sent to the digital input pins of the Arduino. The signals collected by the analog and digital pins of the Arduino were then processed by a C++ code uploaded to the microcontroller which was then output via USB to a laptop running an excel data streamer to tabulate data collected. Full instrumentation set up can be seen in Figure 22.

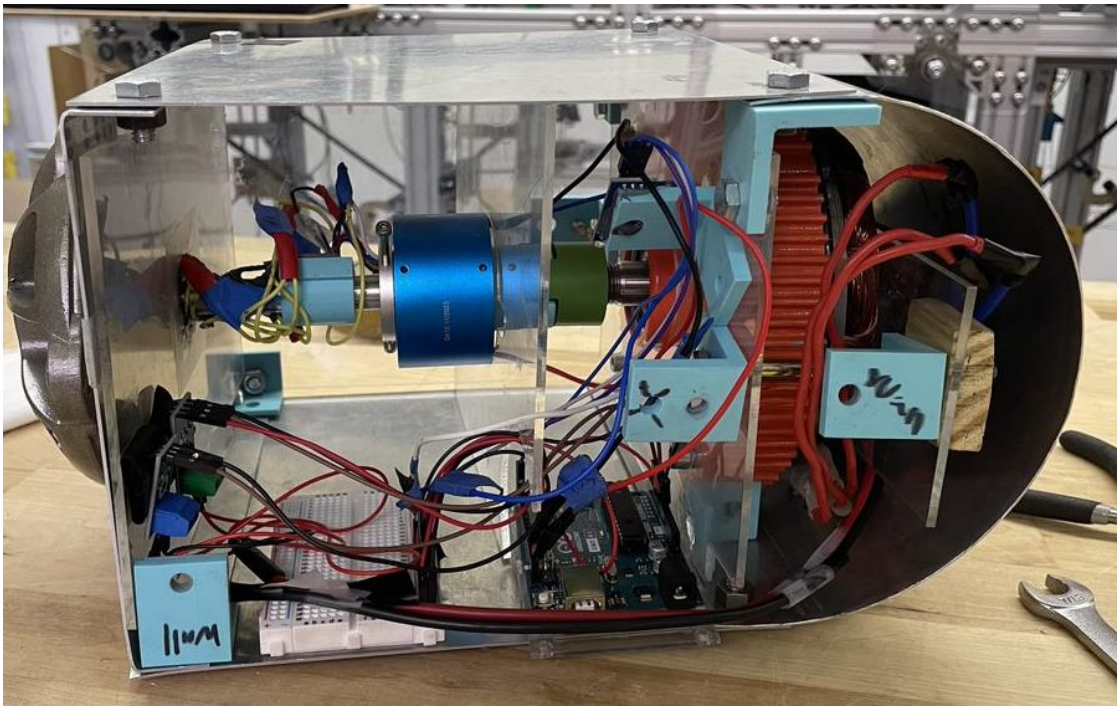

Figure 22: Full Turbine Instrumentation

The code uploaded to the Arduino can be seen in Appendix C: Arduino Code. It is broken up into three sections: variable and function declaration, initialization, and testing loop. The variable and function declaration create variables that will be used to store and calculate desired values from the unprocessed signals collected by the sensors. The initialization function, setup(void), is run once per testing section to create a base line for our Wheatstone bridge. This is done since we were unable to zero the bridge's voltage with hardware.

The testing loop, loop(void), is what collects data during live testing. A timer is established and a check if the code is in calibration mode is run. If in calibration mode, only the Wheatstone bridge output and time is output to assist in calibrating the sensor. This is used to create a calibration curve by hanging known weights from a predetermine length while the generator is fixed in place and comparing it to the output of the Wheatstone bridge. If in testing mode, RPM is first determined by dividing the number of times the IR sensor detected the reflective strip on the generator side by the total time elapsed. This is then multiplied by a time

scaling factor to get the final reading. Next, torque is evaluated by reading the output of the Wheatstone bridge and using the equation from section 2.4 Measuring Torque of a Rotating Shaft. This is then multiplied by the correction factor found during calibration to get the final mechanical torque value. Voltage is found with the voltage read from the junction of the voltage divider. Current is found by averaging the hall-effect sensor's output , subtracting it from the zero point, and dividing that value by a scale factor. The values of voltage and current are then multiplied together to get the power generated by the generator. The last data point that is collected is the comparison torque value which is found by dividing the generated power by the rotational speed of the drive shaft. The last portion of the code is responsible for outputting the data to either the serial monitor or an Excel sheet with data streaming enabled.

4.3 Test and Validate Novel Wind Turbine

The following section will cover our results from wind tunnel testing. Components tested were the modified wind turbine assembly with torque instrumentation and tilting mechanism.

4.3.1 Wind Tunnel Turbine Testing

The first actual testing day for our project to maximize the energy output of a wind turbine using novel designs went reasonably well, though not without some issues. In the first two tests, the turbine blades spun at a normal speed, but we did not get the data we were hoping for. This was due to some torque measurement problems and friction problems we faced during the run. During this test run, we did not have the turbine's base or tilt mechanism; we were using a metal stool as the mechanism's base. During the first run, we got data, but it was very noisy, and should not have produced those results. In the second test run, the wind turbine did not work, and we were unable to record data for the toque. During the third test on the first day the turbine

was not moving and the data that we got was noisy. Since it was not moving the data was not usable.

We encountered several difficulties on the second day of testing for our wind turbine project, which made it impossible for us to accurately assess energy output. During testing, the turbine once more failed to rotate as intended. The turbine's performance was hard to measure since the torque sensor we were using to record output data was not giving us consistent readings, because a mechanical breakdown in the turbine mechanism occurred due to a dislocated jaw coupler linkage forced a premature end to the test.

Our third testing day was more successful than the previous two. Before starting testing, we calibrated the turbine with proper sensors that had been incorporated and we collected data that we could use, but the RPM sensor was not set up yet. Thus, we got some data, but the 3rd testing date wasn't as successful as we would have hoped.

The fourth day of testing our wind turbine design started off well but was cut short by some issues. During Test 1, we had good conditions to collect data but struggled to maintain consistent turbine speed, with the strain gauge output fluctuating. In Test 2, the turbine began to rapidly accelerate after the coupler unexpectedly decoupled. Before we could gather data for Tests 3 and 4, the coupler completely uncoupled again, forcing us to end testing early. While we obtained some useful strain measurements in the first test, the recurring coupler problems prevented more extensive data collection and performance evaluation. Our team then focused on resolving what caused the rapid acceleration and unexpected decoupling. We also troubleshooted the inconsistent turbine speed and analyzed the data acquired from the brief period of stable operation. This fourth round provided key insights despite the challenges. From these tests, we processed the data collected and were able to produce Figure 23 and Figure 24. Besides the

gradual increase in mechanical power as the fan frequency increases, there is a significant amount of noise in the averaged data line. Between these two figures, the highest average mechanical power output was during test two at 1.2 Watts with a horizontal speed of about 3.17 m/s (7 mph).

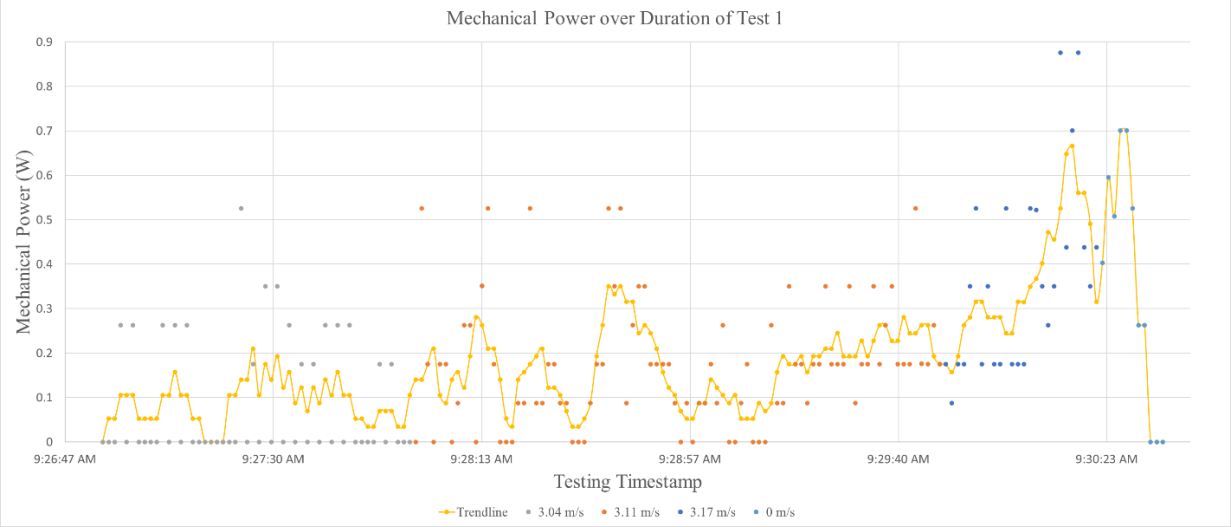

Figure 23: Mechanical Torque Data 1

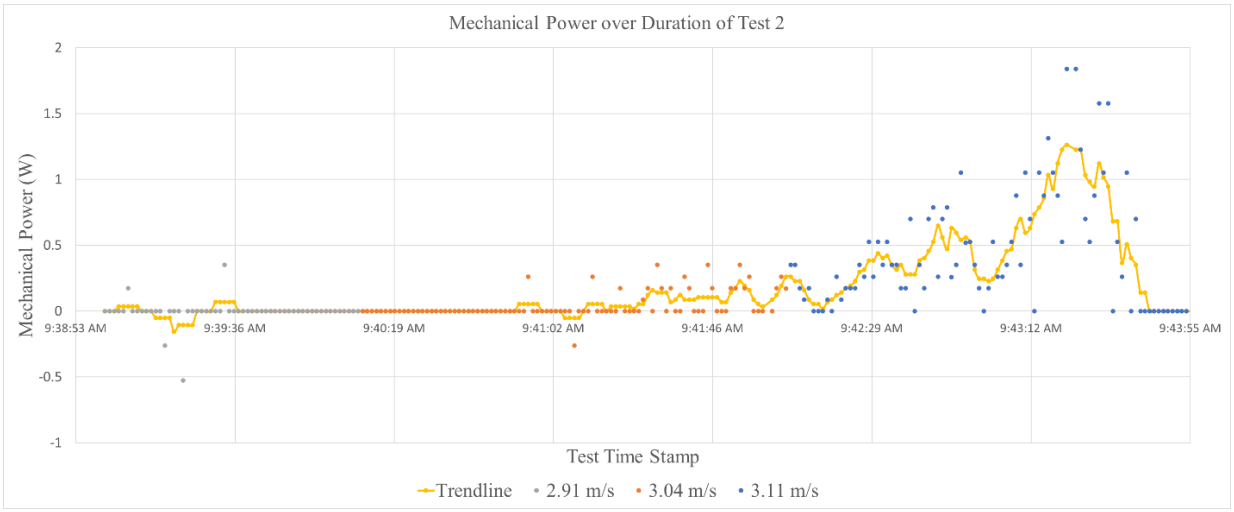

Figure 24: Mechanical Torque Data 2

4.3.2 Tilt Mechanism testing

A key component of our wind turbine design is the tilt mechanism that allows adjustment of the turbine's vertical axis orientation. This includes a rotating platform placed behind the

rotating plate that enables it to pivot. That platform rotates using a rotating rod that is connected to each side of the base. To assess the functionality of this mechanism, we conducted a series of tests at Higgins Lab utilizing an industrial fan to simulate thermal currents. Throughout the experimentation process, we adjusted the orientation of the fan to mimic various wind vector angles. As we manipulated the fan's angle, our tilting mechanism responded by repositioning itself in accordance with the degree of interaction it experienced from these airflow patterns.

Figure 25: Tilting Mechanism Testing

Moreover, to measure the wind speed contacting the wing, we used a hand anemometer and for tracking the angle of the fan and the tilt mechanism, we employed the gyroscope integrated into our mobile devices, yielding the data showcased in Figure 26. Within this figure, we emphasize the wind speed directly influencing the wing, the fan's inclination in 10-degree

intervals, and the measured tilt angle of our tilting mechanism resulting from the air's interaction with the wing. Through this experiment, we observed that the results extracted from the testing were not 100% accurate. As illustrated in Figure 26, as we inclined the fan, the wind contacts with the wing decreased. We hypothesized that this was due to the fan's conical shape of producing wind, creating a void in the middle, potentially impacting the fan's effectiveness at 30°, where significant contact with the wind speed was not achieved. Nevertheless, as we continued to adjust the fan, we observed that an angle of 50° provided the optimal performance from our tilting mechanism. This trial proved invaluable in comprehending the functionality of our mechanism while mimicking thermal effects.

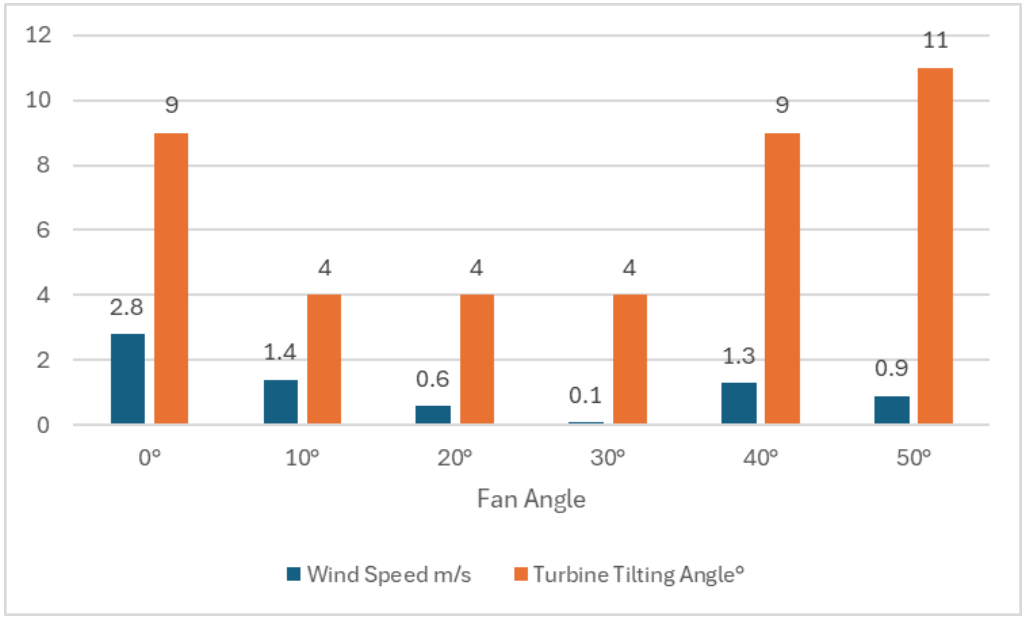

Figure 26: Tilting Mechanism Testing Data

5. Discussion

The following section will discuss the shortcomings our team faced during the project. First the instrumentation is discussed, followed by vibration of the turbine. Next is the tilting mechanism and then the mast.

5.1 Instrumentation

Although the sensors installed in the turbine were able to measure a number of data points from the turbine, there were still some limitations our group faced with them. One of larger problems faced was the significant amount of noise coming from the mechanical torque data. In static orientations, the sensor is able to reliably produce the same measurement over multiple instances. However, when it came to the dynamic torque testing, the data collected was noisy and required a significant amount of processing in order to collect usable data from the test. Another issue that was discovered was occasionally the sensor was found to have voltage stick between measurements. This would cause the sensor to occasionally begin to produce correct readings and add to the noise in the data, which was especially apparent when there was no load acting on the driveshaft.

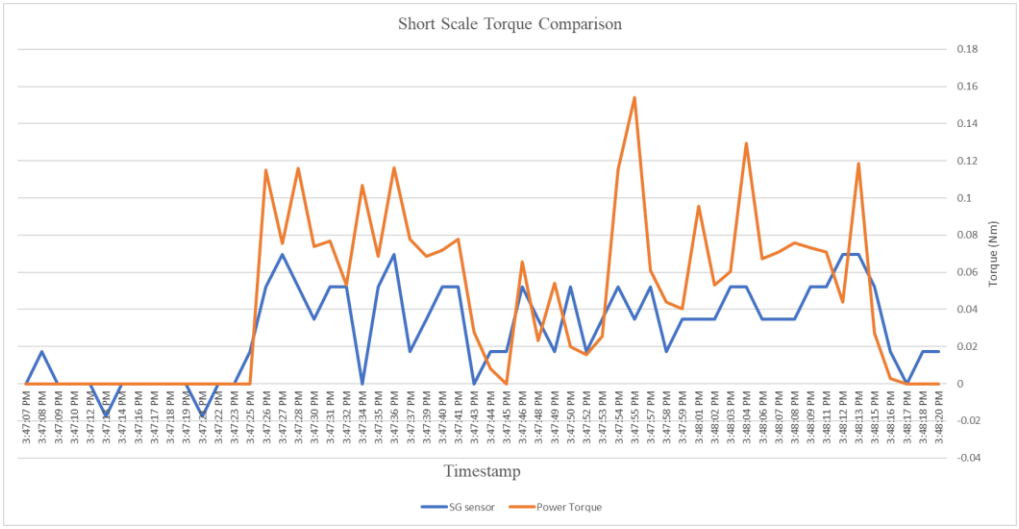

Figure 27: Torque Sensor Noise

In addition to the torque sensor, the method of collecting current data was not the best. Given the construction of the Nacelle, it may have not been the best choice to use a current sensor based on the Hall effect in side an Aluminum enclosure in close proximity to a generator. This resulted in the data having the current sensor never have an exact reading of zero amperes.

The tachometer had minor problems regarding measurement consistency. At times, the RPM values can be seen jumping between extreme values. This may be due to the combination of the reflective strip used to count rotations being too large and the driveshaft not rotating fast enough to have consistent readings.

One final point of discussion for the instrumentation is collecting wind speed data and event tracking. The way our group achieved this was through manual collection via hand-held anemometers and written time stamp recordings to be compared to video recordings. This is another shortcoming of this project since it introduced a significant amount of human error into the data, at certain points having unusable data due to mishandling or miscommunication.

5.2 Turbine Vibration

Different parts of the assembly vibrated while operating, causing small energy losses. There was a significant amount of the small energy losses that the current design sometimes needs small physical pushes to begin operation. When in motion, we must be careful as to how fast we allow the turbine to spin. As the blades accelerate, vibrations become increasingly violent and the lack of a braking system left no other choice but to either cut all simulated wind streams, or physically stop the turbine from spinning. We viewed these vibrations to be emanating from all components of the turbine, especially in the mast and nacelle.

5.3 Tilt Mechanism

Due to the positioning of the current design of the tilt mechanism, there were several current issues. While building this mechanism, we noticed that the system's wide structural framework created vibrations, which we believe could be mitigated with adequate springs or dampers to isolate sensitive components. These vibrations compromise the stability of the entire mechanism, impacting the performance of our instrumentation leading to errors, and diminishing the overall productivity of the system.

Furthermore, our current tilt mechanism cannot fully angle itself to the theoretical 30° angle. This issue may be attributed to the structural balance of the entire turbine, which leads us to the next observation. Our wind turbine currently possesses a plate called the Wing, where all the lift is produced. Accounting for an increase in the plate "wing" area effectively enhances lift but also introduces new structural defects. This alteration shifts the turbine's current center of gravity (CG) position and could demand a reconfiguration of mass balance, crucial for the tilting mechanism's proper functionality. Therefore, ensuring that all masses align at the same center of gravity point is imperative for optimal and stable operation of the tilting mechanism within the turbine.

5.4 Mast

The mast, as observed during the assessment, possessed a distinctly rudimentary appearance, heavily reliant on screws and brackets for its structural integrity. Essentially all connections between various components were secured with screws, making any form of manipulation, be it assembly, disassembly, or addition of components, an arduous and time-consuming task. Managing the multitude of screws, ensuring none were misplaced, and maintaining a backup inventory added an additional layer of complexity to the mast's design.

These challenges were particularly evident during testing sessions, where the turbine necessitated disassembly for safe transfer to Gateway and subsequent reassembly on-site. On average, this process consumed approximately thirty minutes from arrival at Gateway to the initiation of testing.

Despite the inclusion of base supports aimed at dampening mast vibrations since the project's initiation, noticeable vibration persisted. Predominantly, vibrations were concentrated towards the mast's upper section, near the nacelle, specifically along its yaw axis. Consequently, turbine testing had to be conducted at reduced speeds, undermining the effectiveness of evaluating turbine power output.

Furthermore, the current base support comprised wooden 2x4s, which, despite providing some level of rigidity to the mast, exhibited slight vibrations when the turbine was in motion. This vibration led to the galling of screws used to fasten the wood to the base. Consequently, the screws were less effective in securing the wood, thereby allowing for increased clearance and movement of the wooden pieces. In summary, the primary concerns regarding the mast centered on issues of stability and vibration.

6. Conclusion

The goal of this project was to design, fabricate, and test novel wind turbines to maximize energy output. We were able to do this for one of the turbines, which utilized a tilt-mechanism to change the pitch of the turbine's nacelle. The turbine's tilting mechanism was seen to work in the tests we conducted and adjusted according to our simulated vertical wind vectors. The blades would rotate according to horizontal wind vectors, confirming that the unorthodox turbine setup could produce a mechanical motion. From this motion, we obtained readings from our various sensors and generator via the Arduino, of which we could confirm that an electrical output was being produced. However, the current design is still in its primary stages and far from an optimized design. It would also be wrong to say we obtained prime testing results. The entire assembly suffers from severe vibration, leading to visible noise throughout our data. This vibration is not ameliorated by the fact our design has no incorporated braking system. The fastest way to stop the turbine as it currently is, is physically. The data we obtained showed extremely low efficiency, with heavy noise and a maximum power output of ~1.9 W as seen with our second test.

We are not saying, however, that the project was a failure. We have confirmed the tilt mechanism, the aspect which sets this turbine apart from others. This, and the current turbine assembly, sets the base for what future MQP teams will work with. Further on, we will provide a comprehensive list of what these teams can work on to improve the turbines design/configuration. Moving into applications this turbine can take, it will ideally be placed in urbanized areas, or industrial areas. This may come in the form of setting a group of turbines in a parking lot, where the black pavement can provide the thermals needed to tilt the nacelle. Placing them alongside highways is another potential location for them. The size of a typical model can

vary, but we are looking for a mid-range sized model; the original design assumed a mast height of ~20 ft. On the impact of the project itself, it utilizes a concept that hasn't been considered for the design of wind turbines. By making sure the resulting nacelle adjusts parallel to the resulting wind, we are also ensuring that the blades will remain perpendicular. This in turn creates a more efficient power output than traditional turbine designs. In a general move towards more clean forms of energy, this is an aspect which should not be looked past. Better energy efficiency will reduce the dependency on nonrenewable energy sources.

7. Broader Impacts

The broader impact of this project can be seen in the potential energy and environmental gains once this prototype becomes fully mature. Going back to the turbine theory from section 2.3 Design and Operational Parameters of Wind Turbines and using an average horizontal wind speed of 4 m/s (WINDExchange, 2012) and vertical wind speed of 2.5 m/s generated by thermals (Allen, 2006), we expect a 1.5 times performance increase if the nacelle properly oriented into the resultant thermal wind from a single turbine. The potential gains from scaling this design to a small farm scale will have significant impact on energy production, especially in more rural and disconnected communities. Installation of a mature form of this design can help with grid stability and energy security in areas prone to thermal winds. A small farm will assist in localization of power generation, will reduce the reliance on centralized power stations which can affect a large amount of people if an outage occurs. The small farm can also bring power to communities in places were connecting to the power grid is not feasible or impossible.

In addition to the energy impacts, full maturity of this technology will also reduce the overall environmental impact of power generation. As of 2022, 56% of electricity generation was produced through fossil fuels like natural gas and coal whereas wind only made up 10% (LLNL 2023). With improvements to wind technology, through developments like this project, in conjunction with improved energy storage technology, society as a whole can reduce the reliance on fossil fuels. Wind turbines and other renewable energy sources can generate energy based on their operation conditions and be used or stored for later use. When needed, stored energy can be drawn from these energy storage units instead of burning fossil fuels.

8. Recommendations

Although a significant amount of progress was made during the course of this project, there are many improvements that can be made to further improve the current turbine design. This section will highlight key aspects our team believes will improve future prototypes of this turbine design.

8.1 Instrumentation

In order to collect more data to make better design improvements, our team recommends a number of points that will assist in this effort. The first would be looking at improving the SG torque sensor. As mentioned in the discussion, noise with this data was a significant difficulty our team faced with this sensor. To address this, we would recommend looking into less noisy signal transmission. This can be done with high quality slip rings or looking into wireless data transmission. Wireless data transmission could help reduce data noise at the cost of latency. In addition, looking into the voltage sticking phenomenon from the sensor would also improve the sensor's efficacy. One way that could fix this problem would be by developing a way to zero the bridge with hardware versus the software work-around our team used.

To improve power measurement data quality, looking into applying real loads like batteries or light sources should be used to give a better demonstration of power generation. The current turbine does not feature these functions and is only able to display power readings through the Arduino instrumentation output. This would also allow for wattage meters to be used for additional data points for analysis.

To improve environment conditions data, we recommend the addition of three anemometers affixed in the following locations: mast body, nacelle body in front of the blades, and under the wing. The type of sensor we recommend would be the Wind Sensor Rev C by

Modern Device since it can accurately measure wind velocity independent of direction. For the mast mounted sensor, it would be placed in front of the turbine to collect ambient wind velocity. It would also need a wind vain capable of recording the direction of the wind in all four cardinal directions as well as the angle of the incoming wind for thermals direction measuring. The sensors mounted in front of the turbine blades will help measure the incoming wind speed and help with turbine efficiency calculations. The final sensor under the wing will help collect the vertical wind speed providing lift for the tilting mechanism. This sensor will need a shroud to protect against any horizontal wind while the turbine is tilting.

As covered in the discussions, the tachometer can also be used to collect more consistent data. A shroud should be made of a non-IR reflective material to prevent any stray reflections interfering with the tachometer. In addition, more tracking points can be used to increase the number of point the sensor can count during it's one second counting period. These extra tracking points would then be divided out prior to outputting the final RPM reading. The tracking points can also be made thinner to prevent inaccurate readings at lower RPMs.

The final instrumentation recommendation would be a mechanism to record human triggered events with the Arduino. This would reduce the human error of looking at a synchronized clock, writing down that information, and then translating it into the data during post processing. A device as simple as a button flag trigger will greatly increase the accuracy of event logging as only the event order will be needed to be kept track off.

8.2 Tilt Mechanism

To optimize the performance of the tilting mechanism, we recommend prioritizing the center of gravity (CG) optimization and weight reduction measures. It is crucial to conduct a thorough analysis of the mechanism's CG and make the necessary adjustments to redistribute

weight that will enhance the stability and functionality of the whole tilting mechanism. Also, the next team should focus on lightweight individual components through material selection, streamlined design, and integrated component design strategies.

To address the excessive vibration experienced by our turbine, we recommend implementing vibration damping measures. This could involve the installation of dampers or vibration isolation mounts strategically placed throughout the turbine structure. Also, the use of vibration-absorbing materials such as rubber pads can help to mitigate vibrations and improve the overall stability of the system.

Lastly, by transforming the conventional plate or wing into a solar panel we could enhance energy harvesting capabilities. This proposed adaptation not only aligns with the primary objective of the turbine's tilting mechanism but also leverages the same plate to interact with thermal currents while simultaneously harnessing solar energy.

8.3 Mast and Structural Support

To make the mast better we recommend using cheaper, light, and strong material to compose the mast. There are a few materials which come into play, and future teams working on this turbine might want to weigh their options, based on the previously stated desired characteristics. Options for this include PVC, as well as carbon fiber, but once again, we leave this decision for the next team to decide upon. We talked about the wooden supports attached to the feet of the mast and dampen vibrations in the mast as the blades move. Future projects should focus on replacing these supports with a metal or polymer both for better structural integrity and to be more aesthetically pleasing.

We also encourage looking at solutions past the current mast-base's cross-like design, as a more covered surface area will increase the assembly’s stability. Touching once more on the

problems we encountered with the mast, we noticed substantial vibration about the support beams' yaw-axis. This problem could be solved with the change of assembly materials, but if not, the next team should look at ways to dampen vibration throughout the entire height of the mast. Finally, when looking at the assembly process itself, the long time it takes to assemble and disassemble is highly correlated with the number of fasteners that connect parts of the mast together. Finding a way past the need for all these screws means a quicker assembly time as well as reducing weight.

8.4 Nacelle Improvements

The next component that needs to be integrated into the turbine would be adding the yaw control to the nacelle support structure. This was left out in this project in order to focus on the pitch tilting mechanism. This yaw control system would consist of a rotating table that connects the nacelle pivot holder to the mast assembly as well as stabilizer fins to orientate the turbine downwind passively.

Due to design simplifications to reduce complexity, some systems were left out in the current prototype of the turbine. One of these systems is a turbine braking system. On most larger scale turbines, braking systems are common in order to stop operation of the turbine (Manwell et al., 2010). During operation of the current turbine, our team did not let it pick up a significant amount of speed to prevent catastrophic failure. A braking system can greatly improve the testability and safety of the turbine, especially open environment test where the wind speeds are not adjustable like in a wind tunnel test. In situations where mechanical failure occurs, a brake will help quickly slow down rotating machinery so repairs and redesigns can be made appropriately.

One final system that was left out that should be explored are vibration sensing and suppression systems. As previously mentioned throughout the paper, vibration are harmful to the efficiency, structural integrity, and safety of wind turbines. Sensing and suppression systems, be it active or passive, will improve the efficacy of the current turbine by reducing the energy losses due to vibration of turbine components. This will also make the turbine last longer in especially unpredictable conditions that wind turbines are exposed to.

References

Allen, M. (2006). Updraft model for development of autonomous soaring uninhabited air vehicles. In 44th AIAA Aerospace Sciences Meeting and Exhibit (p. 1510).

Angevine, W. M. (2006). Thermal Structure and Behavior. *RC Soaring*.

Annoni, J., Scholbrock, A., Churchfield, M., & Fleming, P. (2017). Evaluating tilt for wind plants. In 2017 American Control Conference (ACC) (pp. 717-722). IEEE.

Boresi, Arthur P. Schmidt, Richard J. (2003). *Advanced Mechanics of Materials (6th Edition) - 2.8.2 Strain-Displacement Relations for Orthogonal Curvilinear Coordinates.* John Wiley & Sons.

De Waal, R. J. O., Bekker, A., & Heyns, P. S. (2018). Indirect load case estimation for propeller-ice moments from shaft line torque measurements. *Cold Regions Science and Technology*, *151*, 237-248.

Co., C. F. (2022, May 22). *Forged vs. cast - What's the difference? - Cornell forge Co*. Cornell Forge Co. https://www.cornellforge.com/blog/forged-vs-cast-whats-the-difference/

García, A., & Partl, M. N. (2014). How to transform an asphalt concrete pavement into a solar turbine. *Applied Energy*, *119*, 431-437.

He, R., Sun, H., Gao, X., & Yang, H. (2022). Wind tunnel tests for wind turbines: A state-of-the-art review. *Renewable and Sustainable Energy Reviews*, *166*, 112675.

Hibbeler, R. C. (2010). *Mechanics of Materials (8th Edition)*. Pearson Education.

Hoffmann, K. (2001). Applying the wheatstone bridge circuit. *Hottinger Baldwin Messtechnick GmbH.*

Kang, H. S., & Meneveau, C. (2010). Direct mechanical torque sensor for model wind turbines. *Measurement Science and Technology*, *21*(10), 105206.

Kanoglu, M., Cengel, Y. A., Cimbala, J. M. (2019). Fundamentals and applications of renewable energy. McGraw Hill Professional.

Leishman, J. G. (2022). Aerodynamics of Airfoil Sections. In *Introduction to Aerospace Flight Vehicles* (1st ed.). https://doi.org/https://doi.org/10.15394/eaglepub.2022.1066.n23

LLNL. (2023). Estimated U.S. energy consumption in 2022: 100.3 quads. US Department of Energy and Lawrence Livermore National Laboratory.

Manwell, J. F., McGowan, J. G., & Rogers, A. L. (2010). Wind energy explained: theory, design and application. John Wiley & Sons.

Office of Energy Efficiency & Renewable Energy. (n.d.). *How do wind turbines work?* Energy.gov. Retrieved April 20, 2024, from https://www.energy.gov/eere/wind/how-do-wind-turbines-work

Schicker, R. & Wegener, G. (2002). Measuring Torque Correctly. *Hottinger Baldwin Messtechnik.*

Slaughter, W. S. (2002). *The Linearized Theory of Elasticity* (1st ed. 2002.). Birkhäuser Boston. https://doi.org/10.1007/978-1-4612-0093-2

U.S. Energy Information Administration (EIA). (2023, April 20). *Electricity generation from wind*. Retrieved April 20, 2024, from https://www.eia.gov/energyexplained/wind/electricity-generation-from-wind.php

U.S. Energy Information Administration (EIA). (2023, March 2). *Frequently asked questions (FAQs)*. Retrieved April 20, 2024, from https://www.eia.gov/tools/faqs/faq.php?id=427&t=3

WINDExchange: U.S. Average Annual Wind Speed at 30 Meters. (n.d.). Windexchange.energy.gov. https://windexchange.energy.gov/maps-data/325

WINDExchange. (2012). U.S. Average Annual Wind Speed at 30 Meters. Windexchange.energy.gov. https://windexchange.energy.gov/maps-data/325

Zhou, X., & Xu, Y. (2016). Solar updraft tower power generation. *Solar Energy*, *128*, 95-125.

Appendix

Appendix A: Derivation of strain gauge deformation to torque on a shaft

Small deformation theory equations adapted from Boresi (2003), Hibbeler (2010), and Slaughter (2002). Strain gauge equation adapted from Hoffmann 2001.

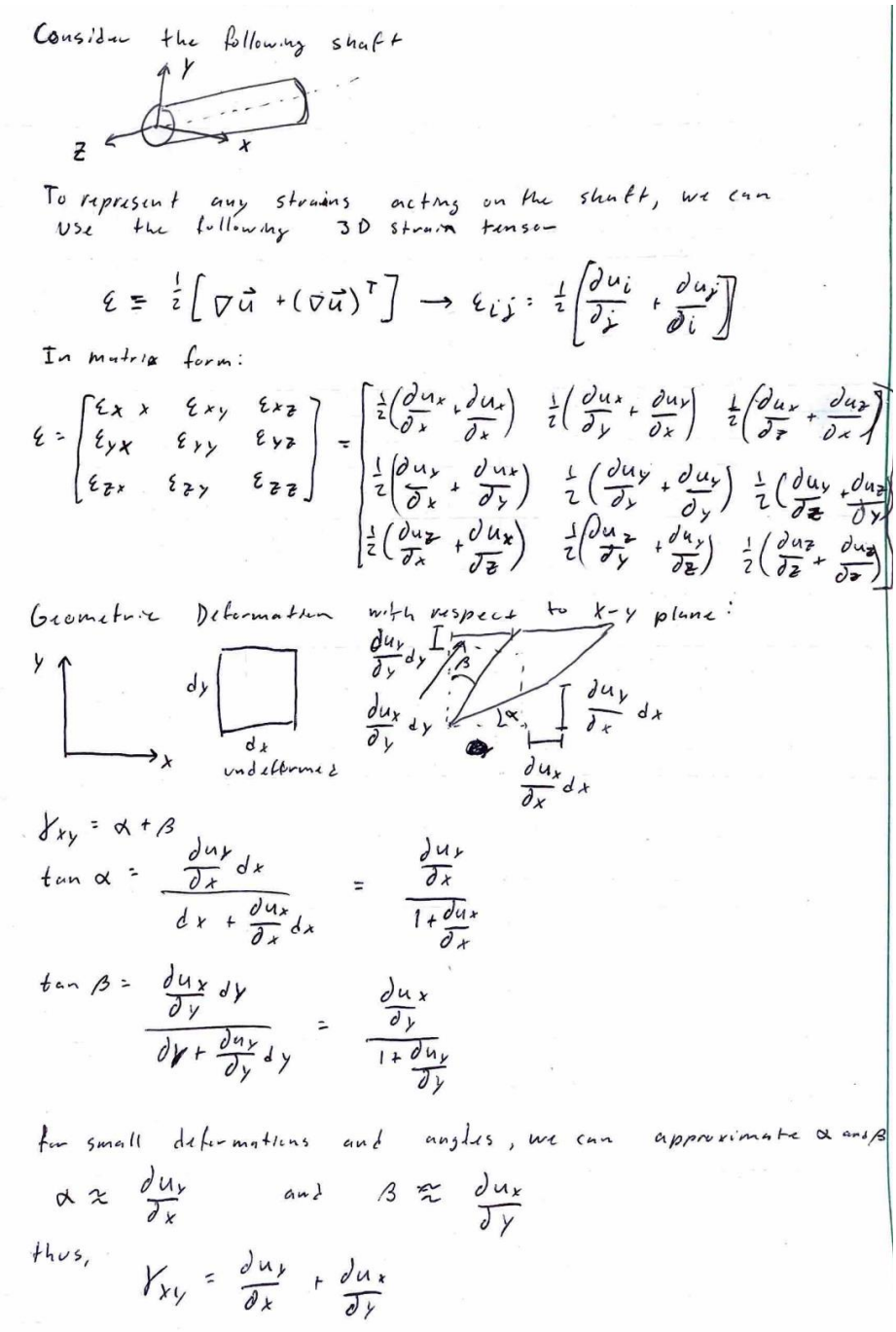

Now ε is:

$$\begin{bmatrix} \frac{\partial u_x}{\partial x} & \frac{1}{2}\gamma_{xy} & \frac{1}{2}\gamma_{xz} \\ \frac{1}{2}\gamma_{yx} & \frac{\partial u_y}{\partial y} & \frac{1}{2}\gamma_{yz} \\ \frac{1}{2}\gamma_{zx} & \frac{1}{2}\gamma_{zy} & \frac{\partial u_z}{\partial z} \end{bmatrix}$$

So $\varepsilon_{xx} = \frac{\partial u_x}{\partial x}$

$$\varepsilon_{yy} = \frac{\partial u_y}{\partial y}$$

$$\varepsilon_{zz} = \frac{\partial u_z}{\partial z}$$

$$\varepsilon_{xy} = \varepsilon_{yx} = \frac{1}{2}\gamma_{xy} = \frac{1}{2}\gamma_{yx}$$

$$\varepsilon_{xz} = \varepsilon_{zx} = \frac{1}{2}\gamma_{xz} = \frac{1}{2}\gamma_{zx}$$

$$\varepsilon_{zy} = \varepsilon_{yz} = \frac{1}{2}\gamma_{yz} = \frac{1}{2}\gamma_{zy}$$

Deriving Torque from torsional shear strain

Wheat stone ~~c~~ circuit.

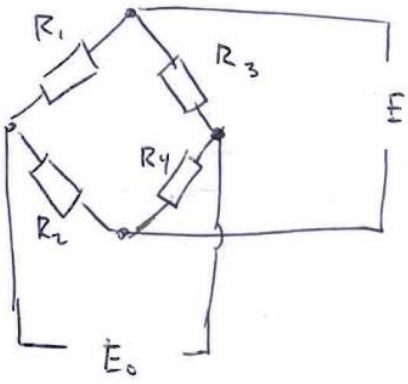

$\frac{E_o}{E_i} = 0$ if $R_1 = R_2 = R_3 = R_4$

$\frac{E_o}{E_i} = \frac{1}{4}\left[\frac{\delta R_1}{R_1} - \frac{\delta R_2}{R_2} + \frac{\delta R_3}{R_3} - \frac{\delta R_4}{R_4}\right]$ for Detuned bridge

$E_o \neq 0$

For strain gauges:

$$\varepsilon = \frac{\delta R/R}{GF} \longrightarrow \frac{\delta R}{R} = \varepsilon \cdot GF$$

$$\frac{E_o}{E_i} = \frac{GF}{4}\left[\varepsilon_1 - \varepsilon_2 + \varepsilon_3 - \varepsilon_4\right]$$

For measurment on a twisting shaft w/ Full bridge.

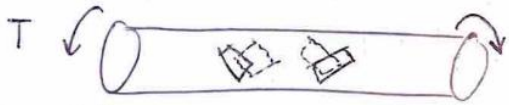

assume $|\varepsilon_1| = |\varepsilon_2| = |\varepsilon_3| = |\varepsilon_4|$

$\frac{E_o}{E_i} = \frac{GF}{4} B \varepsilon$ where B is Bridge factor = 4 for Full bridge.

$\frac{E_o}{E_i} = GF\,\varepsilon \longrightarrow \varepsilon = \frac{E_o}{E_i\, GF}$

Relationship between normal strain and electrical output of wheatstone bridge.

Torsion of circular shaft

Shear strain

$$\gamma = \frac{\theta D}{2L}$$

D = diameter
L = length of shaft
θ = twist angle

twist angle

$$\theta = \frac{TL}{GJ}$$

T = torque
L = length of shaft
G = Shear modulus
J = Polar moment of cross section

$$G = \frac{E}{2(1+\nu)} \qquad J = \frac{1}{2}\pi r^4 = \frac{\pi}{32} D^4$$

$$\theta = \frac{TL}{\frac{E}{2(1+\nu)} \frac{\pi D^4}{32}} = \frac{64(1+\nu) TL}{E \pi D^4}$$

$$\gamma = \frac{\frac{64(1+\nu) TL}{E \pi D^4} D}{2L} = \frac{32(1+\nu) TD}{E \pi D^4}$$

Solve for torque:

$$T = \frac{\gamma E \pi D^4}{32(1+\nu) D}$$

Engineering shear strain

$$\varepsilon = \frac{\gamma}{2} \rightarrow \frac{\gamma}{2} = \frac{E_0}{E_i G_F} \rightarrow \gamma = \frac{2E_0}{E_i G_F}$$

$$\boxed{T = E_0 \frac{E \pi D^4}{16 E_i G_F D(1+\nu)}}$$

Appendix B: Tilt mechanism Free Body Diagram Analysis

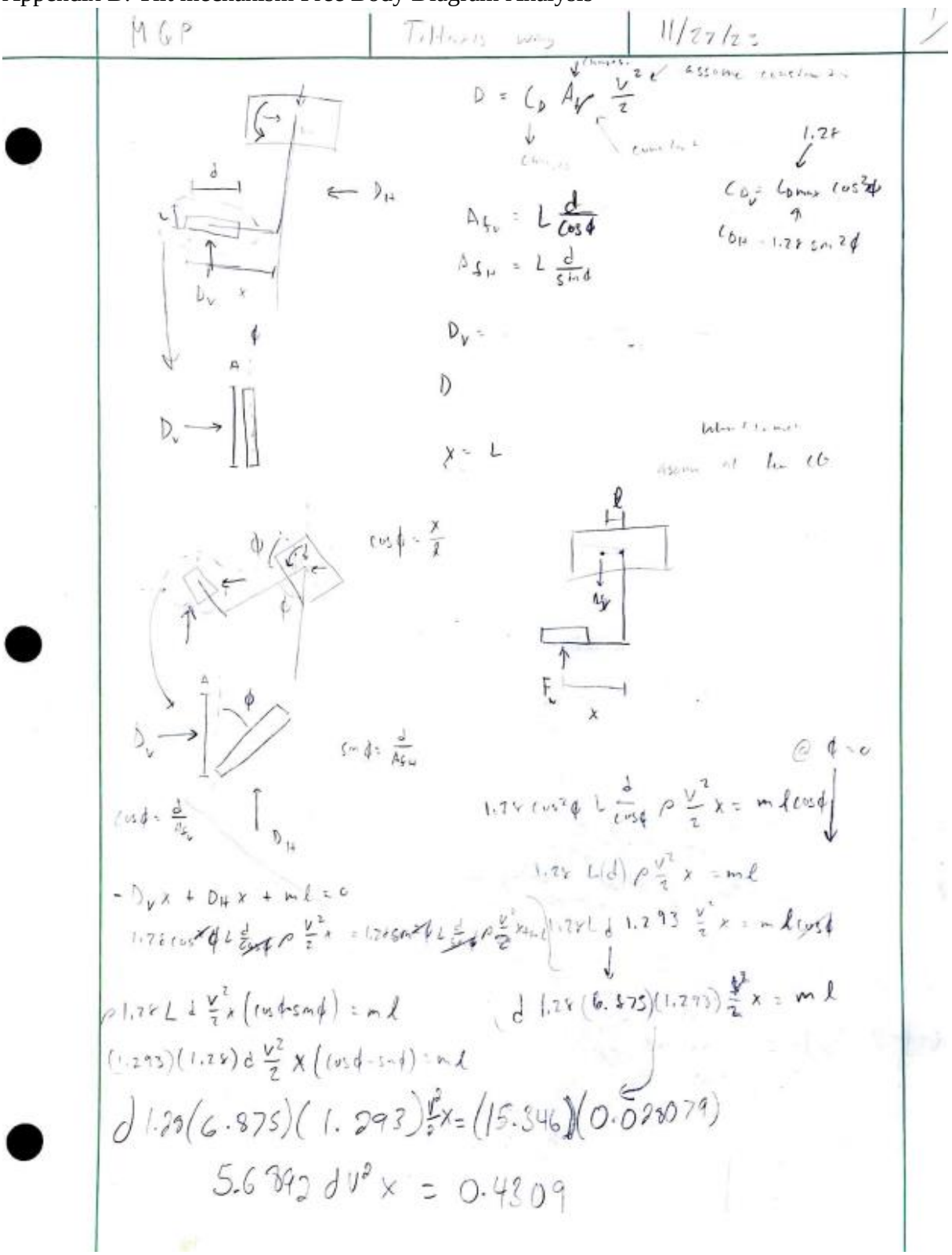

Appendix C: Arduino Code

Below is the code that collects data from individual sensors inside the nacelle. Adapted from ME 3901's stress lab code.

```
#include <Wire.h>
#include <Adafruit_GFX.h>
#include <Adafruit_ADS1X15.h>  // same library for both the ads1015 and ads1115
Adafruit_ADS1115 ads1115;  // Declare an instance of the ADS1115 at address slot 0x48
int16_t rawADCvalue;  // The is where we store the value we receive from the ADS1115
                      //  int16_t is a 16 bit signed integer range = -32768 to +32767
                      // scalefactor = max Voltage /(  (2^15)-1 = max Voltage/(32767) for 16 bit with most
                      //   significant bit reserved for sign (+ or -)
float volts = 0.0;        // The result of applying the scale factor to the raw value
float bit_res = 0.0078125;    //  This is the bit resolution in [mV] will change with the gain, please refer to the table below
float uV = 0.0;           //  This is just volts times a million [uV]
unsigned long StartTime = 0;
float genPower = 0.0;

int calibrationmode = 0; //0 = test; 1 = calibration

//voltage measurment
#define ANALOG_IN_PIN A0
float adc_voltage = 0.0;
float in_voltage = 0.0;
float R1 = 30000.0;
float R2 = 7500.0;
float ref_voltage = 5.0;
int adc_value = 0;

//current measurment
double Vout = 0.0;
double Current = 0.0;
const double scale_factor = 0.1;
const double vRef = 5.00;
const double resConvert = 1024;
double resADC = vRef/resConvert;
double zeroPoint = vRef/2;

//tachometer
float value=0;
float rev=0;
int rpm;
int oldtime=0;
int time;

void isr() //interrupt service routine
{
  rev++;
}

//torque estimation
double comp = 0.0;

//torque constants
double correction = 1.019685;
float E = 73.1*pow(10,9);
float GF = 2.02;
float D = 0.0127;
float v = 0.33;
float ST =0.0;
float startuV = 0.0;
float torqueCorrected = 0.0;

//data smoothing NOT IMPLEMENTED YET
const int numReadings = 10;
int readings[numReadings];  // the readings from the analog input
int readIndex = 0;          // the index of the current reading
int total = 0;              // the running total
int average = 0;            // the average

//                               //  Gain      Max Volt     ads1015          ads1115
// ads1115.setGain(GAIN_TWOTHIRDS);// 2/3x gain +/- 6.144V  1 bit = 3mV (default)  1 bit = 187.5 micro-V
// ads1015.setGain(GAIN_ONE);      // 1x gain   +/- 4.096V  1 bit = 2mV          1 bit = 125. micro-V
// ads1015.setGain(GAIN_TWO);      // 2x gain   +/- 2.048V  1 bit = 1mV          1 bit =  62.5 micro-V
// ads1015.setGain(GAIN_FOUR);     // 4x gain   +/- 1.024V  1 bit = 0.5mV        1 bit =  31.25 micro-V
// ads1015.setGain(GAIN_EIGHT);    // 8x gain   +/- 0.512V  1 bit = 0.25mV       1 bit =  15.625 micro-V
// ads1015.setGain(GAIN_SIXTEEN);  // 16x gain  +/- 0.256V  1 bit = 0.125mV      1 bit =  7.8125 micro-V
//
```

```
void setup(void) {
  Serial.begin(9600);
  ads1115.setGain(GAIN_SIXTEEN);  // Set gain to 16x
  ads1115.begin(0x48);
  //  start a timer
  StartTime = millis();
  //Torque Sensor initialization
  rawADCvalue = ads1115.readADC_Differential_0_1(); // Differential voltage measurement between A0 and A1 on the ADC chip
  volts = rawADCvalue * bit_res; // Convert rawADC number to voltage in [mV]
  uV = volts/1000;
  startuV = uV;
  ST = ((startuV*E*3.14*pow(D,4))/(16*5.0*GF*D*(1+v)))*correction;

  //Tachometer things
  attachInterrupt(0,isr,RISING);  //attaching the interrupt
  pinMode(2, INPUT); //Sets sensor as input

  /*
  //data smoothing
   for (int thisReading = 0; thisReading < numReadings; thisReading++) {
    readings[thisReading] = 0;
  }
  */
  //print start of new test
  Serial.print("New test with a nominal start voltage of ");
  Serial.print(uV,8);
  Serial.print(" and nominal torque reading of ");
  Serial.print(ST,5);
  Serial.println(" ");
  delay(500);
}
void loop(void) {
  //Timekeeping
  unsigned long CurrentTime = millis();
  float ElapsedTime = (CurrentTime-StartTime)/1000.0;

  if (calibrationmode == 1) {
     //for (int i = 0; i <1000; i++){
       rawADCvalue = ads1115.readADC_Differential_0_1(); // Differential voltage measurement between A0 and A1 on the ADC chip
       volts = rawADCvalue * bit_res; // Convert rawADC number to voltage in [mV]
       uV = volts/1000; // Express the voltage in Volts
       float torque = (((uV-startuV)*E*3.14*pow(D,4))/(16*5.0*GF*D*(1+v)));
       float torqueCorrected = torqueCorrected + (torque)*correction;
       delay(100);
     //}
     //torqueCorrected = torqueCorrected/1000;
     Serial.print("Time ");
     Serial.print(ElapsedTime,3);
     Serial.print(" ");
     Serial.println(torqueCorrected,8);
  } else {

    //Tachometer
    detachInterrupt(0);          //detaches the interrupt
    time= CurrentTime-oldtime;        //finds the time
    rpm = (rev/time)*60000;         //calculates rpm
    oldtime = millis();             //saves the current time
    rev = 0;
    attachInterrupt(0,isr,RISING);

    //Torque Measurment
    rawADCvalue = ads1115.readADC_Differential_0_1(); // Differential voltage measurement between A0 and A1 on the ADC chip
    volts = rawADCvalue * bit_res; // Convert rawADC number to voltage in [mV]
    uV = volts/1000; // Express the voltage in Volts
    float torque = (((uV-startuV)*E*3.14*pow(D,4))/(16*5.0*GF*D*(1+v)));
    float torqueCorrected = (torque)*correction;


    //voltage measurment
    adc_value = analogRead(ANALOG_IN_PIN);
    adc_voltage = (adc_value * ref_voltage) / 1024.0;
    in_voltage = adc_voltage / (R2/(R1+R2));
```

```
    //current measurment
    for (int i = 0; i < 1000; i++) {
      Vout = (Vout + (resADC * analogRead(A1)));
      delay(1);
    }
    Vout = Vout / 1000;
    Current = abs((Vout - zeroPoint)/scale_factor);

    //Power Generation
    genPower = in_voltage * Current;

    //Comparison Torque
    if (rpm != 0){
      comp = genPower / (rpm*(3.1415/30));
    } else {
      comp = 0;
    }

    //Data Output
    Serial.print("Time ");
    Serial.print(ElapsedTime,3);

    Serial.print(", Bridge voltage (V)= ");
    Serial.print(uV, 8);

    Serial.print(", Torque measured (Nm)= ");
    Serial.print(torqueCorrected, 8);

    Serial.print(", Voltage (V)= ");
    Serial.print(in_voltage, 3);

    Serial.print(", Current (A) = ");
    Serial.print(Current, 3);

    Serial.print(", Generated power (W) = ");
    Serial.print(genPower,4);

    Serial.print(", RPM = ");
    Serial.print(rpm);

    Serial.print(", Power Torque (Nm) = ");
    Serial.print(comp,8);
    Serial.println();
  }
}
```